Supplementary Appendix

This appendix has been provided by the authors to give readers additional information about their work.

Supplement to: Choi B, Choudhary MC, Regan J, et al. Persistence and evolution of SARS-CoV-2 in an immunocompromised host. N Engl J Med. DOI: 10.1056/NEJMc2031364

SUPPLEMENTARY APPENDIX

Table of Contents

SUPPLEMENTAL RESULTS

Virologic studies

Quantitative SARS-CoV-2 viral load testing, concordant with the clinical NP RT-PCR Ct values, demonstrated a peak of 8.86 $\log_{10}$ SARS-CoV-2 RNA copies/mL from the NP swab on Day 143 (Figure S2, Table S1). Increases in NP viral loads were mirrored by increases in sputum and plasma viral loads.

SARS-CoV-2 whole viral sequencing was performed from two to three NP samples each from within four time points: initial infection (T0: Days 18, 25), first recurrence (T1: Days 75, 81), second recurrence (T2: Days 128, 130), and third recurrence (T3: Days 143, 146, 152). Within the first three time points, the two samples showed identical sequences. By the last time point (T3: Days 143, 146, 152), there was evidence of continued SARS-CoV-2 sequence changes and increasing viral diversification. The phylogenetic results were consistent with viral persistence and disease recurrence,[1,2] rather than re-infection[3,4], as all sequences had a common ancestor and differed from all other sequences from Massachusetts (Figures 1a, S6). Between T0 and T1, 11 nucleotide substitutions (2 synonymous, 9 non-synonymous) and a 9-nucleotide deletion were identified. Between T1 and T2, another 10 nucleotide substitutions (3 synonymous, 7 non-synonymous) and a 1-nucleotide deletion were identified (Figure 1b). Between T2 and T3, 11 nucleotide substitutions (3 synonymous, 8 non-synonymous), a 21-nucleotide deletion (Day 146), and a 3-nucleotide deletion (Day 152) were identified. Non-synonymous nucleotide changes were predominantly in the spike (S) region, which comprises 13% of the SARS-CoV-2 genome, but had 57% of the observed changes. Within the spike region, mutations arose at a disproportionately high rate in the receptor binding domain (RBD), which comprises 2% of the genome, but had 38% of all observed changes.

Previously reported resistance mutations to remdesivir were not detected,[5] and no emerging mutations were identified in the RNA-dependent RNA polymerase gene, despite four courses of remdesivir.

We also compared the viral sequences against previously reported sites of potential resistance mutations against the Regeneron antibody cocktail (Table S3).[6] The Regeneron antibody was given on Day 145. We detected the Q493K polymorphism in sequences from both before and after antibody treatment. This mutation was reported after passage experiments against REGN10933, but not REGN10987. On Day 152, we detected the F486I amino acid change. F486V has been described in passage experiments with REGN10933, but it is unclear what effect, if any, F486I has on antibody resistance. We did not detect the emergence of amino acid changes that could increase the risk of resistance to both antibodies. This is concordant with the steep drop in SARS-CoV-2 viral load after antibody administration. Viral sequences can be located with GISAID accession numbers EPI_ISL_593480, EPI_ISL_593557, EPI_ISL_593558, EPI_ISL_593555, EPI_ISL_593478, EPI_ISL_593479, EPI_ISL_593556, EPI_ISL_593553, EPI_ISL_593554.

Viral infectivity studies were performed using nasopharyngeal swab fluid samples (Days 75, 143). Results were consistent with infectious virus (Figure S7). This is the longest duration of infectious SARS-CoV-2 virus isolated from a patient, reported to date.

Immunologic studies

Immunophenotyping demonstrated low levels of B and plasmacytoid dendritic cells, robust T-cell responses to wild-type SARS-CoV-2 virus, initial IgM seroconversion with delayed IgG and waning IgM/IgA titers, and low levels of neutralizing antibodies. The specificity of the immune response for the mutated form of the virus has not yet been assessed.

Immunophenotyping

Immunophenotyping performed on peripheral blood mononuclear cells (PBMC) from Day 81, compared to age-matched Covid-19 patient controls (Table S4), demonstrated very low total B cells, of which the antibody-secreting subset was predominant (Figure S8). There was a marked reduction in plasmacytoid dendritic cells (pDC). Other

findings included reduced T follicular helper cell (Tfh) and classical monocyte levels compared to age-matched patients with Covid-19 (Figure S8).

SARS-CoV-2-specific T cell proliferation studies

The SARS-CoV-2 T cell proliferation assay from Day 81 demonstrated robust CD4 and CD8 T cell responses to SARS-CoV-2 spike and other structural protein antigens (Figure S9).

SARS-CoV-2-specific (commercial) antibody, SARS-CoV-2-specific antibody isotyping, and SARS-CoV-2-specific neutralizing antibody studies

The patient's clinical SARS-CoV-2 antibody testing with commercial assays showed initial seroconversion to IgM (Day 28) and later IgM and IgG (Days 81, 87). Antibody test of SARS-CoV-2 total immunoglobulins on Day 107 was negative (Figure S2, Table S2).

Additional SARS-CoV-2-specific antibody isotyping and subclass analysis was performed by Luminex assay (Figure S10). The patient's spike (S)- (and to a lesser extent) his nucleocapsid (N)-specific IgG1 titer was delayed, mounting higher titers only starting Day 77, but were then sustained throughout the remainder of his course despite recurrence of viremia at multiple timepoints. His IgA and IgM titers remained high throughout until a concurrent decline in titers against S and receptor binding domain (RBD) on Day 146, just after his third recurrence of infection (Day 143: RT-PCR Ct = 15.6) at which point he was treated with an anti-viral antibody cocktail, remdesivir, high dose corticosteroids (Days 143-153), and ruxolitinib (Day 143). While it is possible that IgA and IgM titers may have decreased in response to this combination of immunosuppression and high dose steroids, the decrease in antibody titer does precede most of the course of high dose steroid, raising the question of whether a drop in IgA and IgM may have been permissive of or exacerbated a rise in viral load. Notably, his SARS-CoV-2-specific IgG1 antibodies do not take into account viral escape from neutralizing antibodies, which may be of additional importance.

SARS-CoV-2-specific humoral responses were evaluated by neutralization antibody pseudovirus assays. Serum collected longitudinally from Days 31 through 87 was tested using pseudovirus expressing full length spike (G614) and 293T/ACE2 target cells. Patient samples demonstrated neutralizing activity, but neutralization was relatively similar across timepoints and significantly lower compared to convalescent positive controls (Figure S11). Additional analyses using a different pseudovirus expressing a cytoplasmic tail-truncated form of the spike (D614) protein and TZM.bl/ACE2 indicator cells showed similar results.

Autopsy and tissue studies

Quantitative SARS-CoV-2 viral load of autopsy samples was highest in the respiratory tract, but viral RNA was also detected in the spleen, heart, and gastrointestinal organs (Figure S4). Using the weight of the organs, we calculated the whole-body burden of SARS-CoV-2 and calculated that 18% of the detected RNA was located outside of the pulmonary system. This is likely a substantial underestimate as only a limited number of extra-pulmonary tissues were studied. Post-mortem exam showed active and remote DAH, with superimposed invasive necrotizing *Aspergillus fumigatus* pneumonia (Figure S5). The thoracic and abdominal lymph nodes showed a dramatic loss of normal architecture without germinal centers and a near absence of viable lymphocytes, and the spleen showed an absence of white pulp.

SUPPLEMENTAL INFORMATION REGARDING CLINICAL COURSE

Initial infection

A patient in his 40s with a history of catastrophic antiphospholipid syndrome (APS), complicated by venous thromboemboli, pulmonary emboli, thrombotic microangiopathy, adrenal hemorrhage, coronary vasculitis, and aortitis, was admitted with fever and nausea. The patient was diagnosed with APS in 1998, 22 years before presentation. Five months prior to presentation, he had been treated for diffuse alveolar hemorrhage (DAH), a rare complication of APS.[7,8] He was on warfarin for therapeutic anticoagulation, hydroxychloroquine, cyclophosphamide, and corticosteroids at prednisone 15 mg daily, and he had recently received rituximab and eculizumab (Figure S1). The patient reported chills, muscle aches and headache three days prior to hospitalization and subsequently developed dizziness, nausea without emesis, mid-central abdominal pain, anorexia and persistent fevers. At the time of initial presentation, he denied a change in his baseline exertional dyspnea on exertion. After two initial negative tests, the patient was diagnosed with Covid-19 by nasopharyngeal (NP) swab SARS-CoV-2 real-time reverse transcription polymerase chain reaction (RT-PCR, Hologic Panther), with a cycle threshold (Ct) of 32.4 (Day 0, Figure S2). Chest computed tomography (CT) showed multifocal ground glass opacities (GGOs) in a peribronchial distribution with subpleural sparing (Figure S3). Lab markers of Covid-19-associated cytokine storm were only modestly elevated (Table S5, Figure S12). He developed an oxygen requirement several days later. He was treated with five days of remdesivir and increased corticosteroids for suspected recurrent DAH. He was discharged on room air (Day 5).

Between Days 6 through 68, he was readmitted three times with abdominal pain and once with fatigue and dyspnea, for a total of 29 inpatient days. He otherwise quarantined alone at home and reported no known sick contacts. He had no pets. Admissions were complicated by hypoxemia concerning for recurrent DAH, for which he received higher doses of corticosteroids (Figures S1-S2). SARS-CoV-2 NP RT-PCRs continued to be positive through day 39, although with increasing Ct values suggesting resolving infection (Figure S1).[9,10]

First recurrence

The patient was readmitted from Days 69 through 91 with hypoxemia, requiring up to 6 liters per minute of oxygen with exertion. He endorsed dyspnea but denied fever, productive cough, hemoptysis, sore throat, chest pain, and malaise. Labs were notable for lymphopenia and thrombocytopenia, but lab markers of inflammation remained modestly elevated (Table S5, Figure S12). Chest CT demonstrated increased multifocal peribronchial and subpleural GGOs with new areas of consolidation and architectural distortion (Figure S3). Transthoracic echocardiogram was normal. Anticoagulation, corticosteroids, hydroxychloroquine, and eculizumab were continued. On Day 72, he had a positive SARS-CoV-2 NP RT-PCR with Ct of 27.6, raising concerns for persistent SARS-CoV-2 and Covid-19 recurrence. The patient was treated with a second course of remdesivir for ten days. Subsequent NP RT-PCRs (Days 87, 88) were negative.

Second recurrence

On Day 105, the patient was readmitted with lower extremity cellulitis. He was on room air at rest. Initial NP RT-PCR Ct was 36.9, and RT-PCR on Days 106 and 107 were negative. Anticoagulation, corticosteroids, hydroxychloroquine, and eculizumab were continued. On Day 111, the patient developed increased oxygen requirements and by Day 126 required high flow nasal cannula and admission to the medical intensive care unit. He received pulse-dose corticosteroids with intravenous methylprednisolone 1,000 mg for three days and was subsequently maintained on methylprednisolone 1 mg/kg/day. On Day 128, his NP RT-PCR reached a nadir of Ct 32.7, for which he received remdesivir for five days. Subsequent NP RT-PCR (Day 132) was negative.

Third recurrence

The patient continued to have respiratory decline, raising concern for ongoing active DAH. While on corticosteroids, he received three days of intravenous immunoglobulin, intravenous cyclophosphamide, and daily ruxolitinib. On Day 143, NP RT-PCR was positive with Ct of 15.6. On Day 145, the decision was made to pursue

compassionate use of the Regeneron antibody cocktail against the SARS-CoV-2 viral spike protein.[6] Federal Drug Administration and Mass General Brigham institutional review board approval were granted, and the antibody cocktail was administered as a one-time dose of 8 grams of intravenous delivery of two antibodies (REGN10933 and REGN10987). On Day 150, the patient was intubated for ongoing hypoxemia. Bronchoalveolar lavage yielded an NP RT-PCR Ct of 15.8, for which he received another course of remdesivir, and *Aspergillus fumigatus*, for which he received antifungals. Despite these interventions, the patient developed worsening hemodynamics and respiratory failure and died on Day 154.

SUPPLEMENTAL METHODS

Informed consent was obtained from this patient to participate in a Mass General Brigham Institutional Review Board (IRB)-approved Covid-19 observational sample collection protocol. We assessed levels of SARS-CoV-2 RNA in NP swabs, sputum, plasma, and post-mortem organs through a quantitative viral load assay.[11] Whole viral sequencing and maximum likelihood phylogenetic analyses were performed on longitudinal NP swab samples.[12] Viral infectivity studies were performed on NP swab fluid. Immune cell phenotyping included assays for neutralizing antibody titers, SARS-CoV-2-specific T cell activity, and cell surface marker analysis. Full Methods are below.

Nasopharyngeal RT-PCR
Our clinical microbiology laboratory utilized the Hologic Panther Fusion SARS-CoV-2 real-time reverse transcription polymerase chain reaction (RT-PCR) for molecular testing for SARS-CoV-2 in inpatients. The Hologic Panther Fusion RT-PCR targets two regions of the Open reading frame 1ab (ORF1ab) gene that are specific to SARS-CoV-2. A specimen is considered positive if the gene target has a cycle threshold (Ct) of <40. The assay has a comparable limit of detection and was operated using protocols defined by the Emergency Use Authorization.

Quantitative viral load
SARS-CoV-2 viral load was quantified in respiratory samples (nasopharyngeal, sputum) and plasma with a quantitative assay using the US CDC 2019-nCoV_N1 primers and probe set.[13-15] Plasma, sputum, and nasopharyngeal swab fluids were centrifuged at approximately 21,000 x g for 2 hours at 4°C. The supernatant was removed and TRIzol-LS™ Reagent (Thermo Fisher, Waltham, MA, USA) was added to the pellets and then incubated on ice, followed by chloroform (MilliporeSigma, St. Louis, MO, USA). The mixtures were separated by centrifugation at 21,000 x g for 15 minutes at 4°C, and subsequently the aqueous layer was removed and treated with an equal volume of isopropanol (MilliporeSigma, St. Louis, MO, USA). GlycoBlue™ Coprecipitant (ThermoFisher, Waltham, MA, USA) and 100 µL 3M sodium acetate (ThermoFisher, Waltham, MA, USA) were added to each sample and incubated on dry ice until frozen. RNA was pelleted by centrifugation at 21,000 x g for 45 minutes at 4°C. The supernatant was discarded and the RNA was washed with cold 70% ethanol and resuspended in DEPC-treated water. Each reaction contained extracted RNA, 1X TaqPath™ 1-Step RT-PCR Master Mix, CG (ThermoFisher, Waltham, MA, USA), the CDC N1 forward and reverse primers, and probe.[13] Quantification of the Importin-8 (IPO8) housekeeping gene RNA level was performed to determine the quality of respiratory sample collections. An internal virion control (RCAS) was spiked into each sample and quantified to determine the efficiency of RNA extraction and PCR amplification.[16] SARS-CoV-2 viral loads below 40 RNA copies/mL were categorized as undetectable and set at 1.0 $\log_{10}$ RNA copies/mL.

Post-mortem tissue RNA extraction
Frozen tissue samples were thawed on ice and trimmed to a weight of 100mg. Samples were then minced in Trizol (ThermoFisher), homogenized by vortexing, and incubated at RT for 10 minutes. RNA was then extracted with a Direct-zol DNA/RNA miniprep kit (Zymo Research) according to manufacturer's instructions. Total RNA was eluted in a volume of 30 µL nuclease-free water. Extracted RNA was quantified on Nanodrop. Each reaction contained 100ng of extracted RNA, 1X TaqPath™ 1-Step RT-qPCR Master Mix, CG (ThermoFisher), the CDC N1 forward and reverse primers, and probe.[13]

SARS-CoV-2 whole viral sequencing, assembly, and phylogenetic analysis
cDNA synthesis was performed using Superscript IV reverse transcriptase (Invitrogen, Waltham, MA, USA). Whole viral amplification was performed using two amplification strategies to rule out PCR artifacts: 1) the Artic protocol using multiplexed primer pools designed with Primal Scheme generating 400-bp tiling amplicons[17,18] and 2) a 20-amplicon strategy using nested PCR amplification with primer sets generating an amplicon sizes of 1.5-2kb. PCR products from the Artic and 20-amplicon strategies were pooled separately and Illumina library construction was performed using the Nextera XT Library Prep Kit (Illumina, San Diego, CA, USA). Sequence reads were assembled by a customized SARS-CoV-2 module (https://github.com/XuetingQiu/ViralAssembly) within Iterative Refinement Meta-Assembler (IRMA v0.9.3, https://wonder.cdc.gov/amd/flu/irma/), which is designed for highly variable RNA viruses with more robust assembly and variant calling.[19] The SARS-CoV-2 module was created with the generation of a consensus template and reference profile from publicly available whole genome sequences deposited in GISAID (https://www.gisaid.org/).[12] The minimum variant calling frequency was set to be 5% to identify within-

host variations. The resulting DNA libraries were sequenced with the MiSeq instrument (Illumina, San Diego, CA, USA). The comparison dataset included 167 representative SARS-CoV-2 genomes randomly selected from GISAID (Table S6) by regions of interest (Massachusetts, United States, and globally). Furthermore, a representative local viral population containing 552 isolates from Massachusetts and other New England areas (Table S7) was used to provide a higher resolution of potential local clustering. Nucleotide sequence alignment was performed with MAFFT (multiple alignment using fast Fourier transform).[20] Best-fit nucleotide substitution GTR+G+I was used for the datasets using model selection in IQ-Tree followed by maximum likelihood phylogenetic tree construction using IQ-Tree web server with 1000-bootstrap replicates.[21]

SARS-CoV-2 viral infectivity studies

The NP specimens on Days 75 and 143 were thawed on ice and filtered through 0.45 μm Spin-X centrifuge filters (Sigma) at 10,000xg at 4°C for 10 minutes. The filtrate was then diluted 1:10 in D^+ (DMEM (Fisher) supplemented with Penicillin/Streptomycin (Fisher) and Hepes buffer (Fisher)). 200 μL of the diluted samples were added to 150,000 Vero-E6 cells (ATCC) in a 12-well plate. D^+ was used as a non-infected control and USA-WA1 (BEI Resources) as positive control.[22] Each condition was tested in duplicate. The plate was then incubated for 1 hour at 37°C on a platform rocker. After 1 hour, the inoculum was removed and 2 mL of fresh media was added (D+ supplemented with 2% FBS(Sigma)) and the plate returned to 37°C. Wells were observed at 24, 48, 72, and 96 hours post infection for cytopathic effect. Negative controls contained no virus. Positive controls contained NR-52281 SARS-Related Coronavirus 2, Isolate USA-WA1/2020. Pictures taken on a Evos XL Core imaging system (Invitrogen) at 4x magnification.

Immunophenotyping by flow cytometry

Immunophenotyping was performed on 1 million cryopreserved peripheral blood mononuclear cells (PBMCs) that were freshly isolated on Day 81 (after thawing) and freshly isolated PBMC from age-matched (40 to 60 years old) patients with active Covid-19 (Table S4). Prior to antibody staining, Fc receptors were blocked using human FcR blocking reagent (Miltenyi, Bergisch Gladbach, Germany) at a concentration of 1:50 at 4°C for 10 minutes. Cells were surface stained at 4°C, protected from light, using optimized concentrations of fluorochrome-conjugated primary antibodies for 30 minutes as well as live/dead fixable blue stain (Thermo Fisher, Waltham, MA, USA) at a concentration of 1:20 using the following panel of antibodies (clone, manufacturer): CD3 (UCHT1, BD Biosciences), CD4 (SK3, BD Bioscience), CD8 (RPA-T8, BD Bioscience), CD11c (Bu15, BD Bioscience), CD14 (M5E2, BioLegend), CD16 (3G8, BD Bioscience), CD19 (SJ25C1, BioLegend), CD25 (2A3, BD Bioscience), CD27 (L128, BD Biosciences), CD38 (HB-7, BioLegend; HIT2, BD Bioscience), CD45RA (HI100, BD Bioscience), CD56 (NCAM16.2, BD Biosciences), CD57 (NK-1, BD Bioscience), CD62L (DREG-56, Biolegend), CD123 (6H6, Biolegend), CD127 (A019D5, Biolegend), CD138 (MI15, BioLegend), CCR4 (1G1, Biolegend), CCR6 (G034E3, Biolegend), CXCR3 (G025H7, Biolegend), CXCR5 (J252D4, BioLegend; RF8B2 BD Bioscience), CX3CR1 (2A9-1, Biolegend), HLADR (L243, Biolegend), IgD (IA6-2, BD Biosciences), NKG2A (REA110, Miltenyi), NKG2C (134591, BD Bioscience), PD1 (EH12.2H7, BD Bioscience).

Individual cell subsets were defined as the following:
B cell: CD3-CD56-CD19+
mDC: CD3-CD14-CD19-CD56-HLADR+CD11c+CD123low
pDC: CD3-CD14-CD19-CD56-HLADR+CD11c-CD123bright
Monocyte: CD3-CD19-CD56-CD14+
NK: CD3-CD56brtCD16neg/CD3-CD56dimCD16pos/CD3-CD56negCD16pos
CD4 T cell: CD3+CD4+
CD8 T cell: CD3+CD8+
Ab-secreting B cell: CD27+CD38+ (the rest of B cells are non-Ab-secreting)
Plasma cell: CD27+CD38+CD138+
Plasmablast: CD27+CD38+CD138-
Tfh CD4: CXCR3-CXCR5+
Th1 CD4: CXCR3+CXCR5-
Th1Tfh CD4: CCXCR3+CXCR5+
Th2 CD4: CXCR3-CXCR5-CCR4+CCR6-

Th17 CD4: CXCR3-CXCR5-CCR4+CCR6+
Naïve T cell (within CD4 or CD8+ T cells): CD45RA+CD62L+
Tcm (within CD4 or CD8+ T cells): CD45RA-CD62L+
Tem (within CD4 or CD8+ T cells): CD45RA-CD62L-
Temra (within CD4 or CD8+ T cells): CD45RA+CD62L-

Cells were then washed in phosphate-buffered saline (PBS) and fixed with 4% paraformaldehyde for 30 minutes at 4°C. Flow cytometry was performed on a BD Symphony (BD Biosciences, San Jose, CA), and rainbow tracking beads (8 peaks calibration beads, Fisher) were used to ensure consistent signals between flow cytometry batches. FCS files were analyzed, and subsets of immune cells were quantified using FlowJo software (version 10.7.1). Assembly of quantified cell subsets was performed in GraphPad Prism (version 8.4.3).

Immune profile of the study subject was presented with data from additional 11 freshly isolated peripheral blood samples, drawn from inpatients with Covid-19 at Massachusetts General Hospital. This study was performed with the approval of the Institutional Review Boards at Mass General Brigham.

CD4+ and CD8+ T cell Proliferation Assay
SARS-CoV-2-specific T cell proliferation was performed on peripheral blood mononuclear cells (PBMCs) on Day 81. PBMCs from the patient were collected by Ficoll gradient separation from acid citrate dextrose (ACD) tubes. PBMCs were suspended at 1×10^6/mL in phosphate buffered saline (PBS) and incubated at 37°C for 20 minutes with 0.5 μM carboxyfluorescein succinimidyl ester (CFSE; Life Technologies). After the addition of serum and washes with PBS, cells were resuspended at 1×10^6/mL and plated into 96-well U-bottom plates (Corning) at 200 μL volumes. SARS-CoV-2 peptide pools (JPT, Berlin, Germany) for non-structural proteins (NSP5, NSP6, NSP7, NSP8, NSP9, NSP12, NSP15), Spike protein, and other structural proteins (Nucleocapsid, Membrane, Envelope and ORF3A) were added at a final concentration of 1 μg/mL. On day 6, cells were harvested, washed with PBS + 2% fetal bovine serum, and stained with Alexa Fluor 700 mouse anti-human CD3 antibody (1:200; clone OKT3; BioLegend), APC mouse anti-human CD8 antibody (1:200; clone RPA-T8; BioLegend), PE-Cy7 mouse anti-human CD4 antibody (1:200; clone RPA-T4; BioLegend) and LIVE/DEAD violet viability dye (1:1000; Life Technologies). Cells were washed and fixed in 2% paraformaldehyde, prior to flow cytometric analysis using a BD LSR II (BD Biosciences). Flow cytometric data were analyzed using FlowJo software (v10.1r5).

Quantitative SARS-CoV-2-specific antibodies
Epitope Diagnostics EDI Novel Coronavirus COVID-19 IgM and IgG Enzyme Linked Immunosorbent Assays (ELISA) were performed as per manufacturer instructions (Epitope Diagnostics, San Diego, CA).
Roche Elecsys was performed as per manufacturer instructions (Roche, Basel, Switzerland).

SARS-CoV-2-specific neutralizing antibody assay
Neutralizing activity against SARS-CoV-2 pseudovirus was measured using a single-round infection assay in human ACE2 expressing target cells. Pseudotyped virus particles were produced in 293T/17 cells (American Type Culture Collection) by co-transfection of plasmids encoding codon-optimized SARS-CoV-2 full-length Spike (containing G at position 614), packaging plasmid pCMV ΔR8.2 expressing HIV-1 gag and pol, and luciferase reporter plasmid pHR' CMV-Luc. Plasmids were kindly provided by Dr. Barney Graham (NIH, Vaccine Research Center). This pseudovirus strain was used for infecting 293/ACE2 target cells. A second pseudovirus strain was produced in 293T/17 cells by co-transfection of plasmids encoding codon-optimized Spike (containing D at position 614) with a deleted cytoplasmic tail (provided by Dr. Dan Barouch, Beth Israel Deaconess Medical Center), and the HIV-1 backbone vector SG3Δ Env (NIH AIDS Reagent Program). This pseudovirus strain was used for infecting TZM.bl/ACE2 target cells which encode an integrated luciferase reporter gene under control of an HIV-1 LTR. The 293T and TZM.bl cell lines stably overexpressing the human ACE2 cell surface receptor protein were kindly provided by Drs. Michael Farzan and Huihui Ma (The Scripps Research Institute). For neutralization assays, serial dilutions of patient serum samples were performed in duplicate followed by addition of pseudovirus. Plates were incubated for 1 hour at 37°C followed by addition of 293T/ACE2 or TZM.bl/ACE2 target cells ($1x10^4$/well). Wells containing cells + pseudovirus (without sample) or cells alone acted as positive and negative infection controls, respectively. Assays were harvested on day 3 using Promega Bright-Glo luciferase reagent and luminescence detected with a Perkin-

Elmer Victor luminometer. Titers were determined as the serum dilution that inhibited 50% or 80% virus infection (ID_{50} and ID_{80} titers, respectively).

SARS-CoV-2-specific antibody isotype and subclass analysis via Luminex

Antigen-specific antibody isotype and subclass were evaluated using a previously-described 384-well based customized Luminex assay.[23] Antibody was evaluated longitudinally using serum samples collected on days 31, 59, 73, 77, 81, 83, 87, 131, 133, 146, and 152. The Luminex assay is sample-sparing and amenable to multiplex format, so samples were run in duplicate in a multiplex plate format. Relative antibody concentration was measured against a panel of SARS-CoV-2 antigens. Fluorescent carboxyl-modified microspheres (Luminex) were coupled with different antigens: SARS-CoV-2 spike protein (S) (kindly provided by Bing Chen), SARS-CoV-2 receptor binding domain (RBD) (kindly provided by Aaron Schmidt), SARS-CoV-2 nucleocapsid protein (N) (Aalto Bio Reagents), and recombinant ebolavirus glycoprotein (negative control, Recombinant EBOV GPDTM (mammalian), IBT Bioservices, 0501-001). Luminex bead regions were coupled via covalent NHS–ester linkages utilizing EDC [1-ethyl-3-(3-dimethylaminopropyl) carbodiimide hydrochloride] (Thermo Scientific) and sulfo-NHS (Thermo Scientific) according to the manufacturer's instructions. Antigen-coated microspheres (1.2×10^3 per Luminex region) were added in Luminex assay buffer containing 0.1% bovine serum albumin (BSA) and 0.05% Tween 20 in a 384-well plate (Greiner Bio-one). Five microliters of diluted plasma samples or phosphate-buffered saline (PBS) for background assessment (IgG_1 at 1:500 dilution, other subclasses/isotypes at 1:100) was added in duplicate and incubated with antigen-coated microspheres for 12 h at 4°C while rocking at 900 rpm. The immune-complexed microspheres were washed with an automated plate washer (Tecan). Secondary phycoerythrin (PE)-coupled IgG1-, IgA1-, or IgM-specific detection reagents (Southern Biotech) were added at 1.3 μg/ml in Luminex assay buffer and incubated for 1 h at room temperature while shaking at 900 rpm. The coated beads were washed and read using flow cytometry on an iQue Screener (Intellicyt) with a robotic arm (PAA). Analysis was performed using ForeCyt software to gate on fluorescent bead regions and PE median fluorescent intensity (MFI) which is the reported readout for these relative antibody titers. Samples were run concurrently with convalescent patient serum samples with known high antibody titers and known low/negative antibody titers as controls.

SUPPLEMENTAL FIGURES

Figure S1: Clinical course and immunosuppression

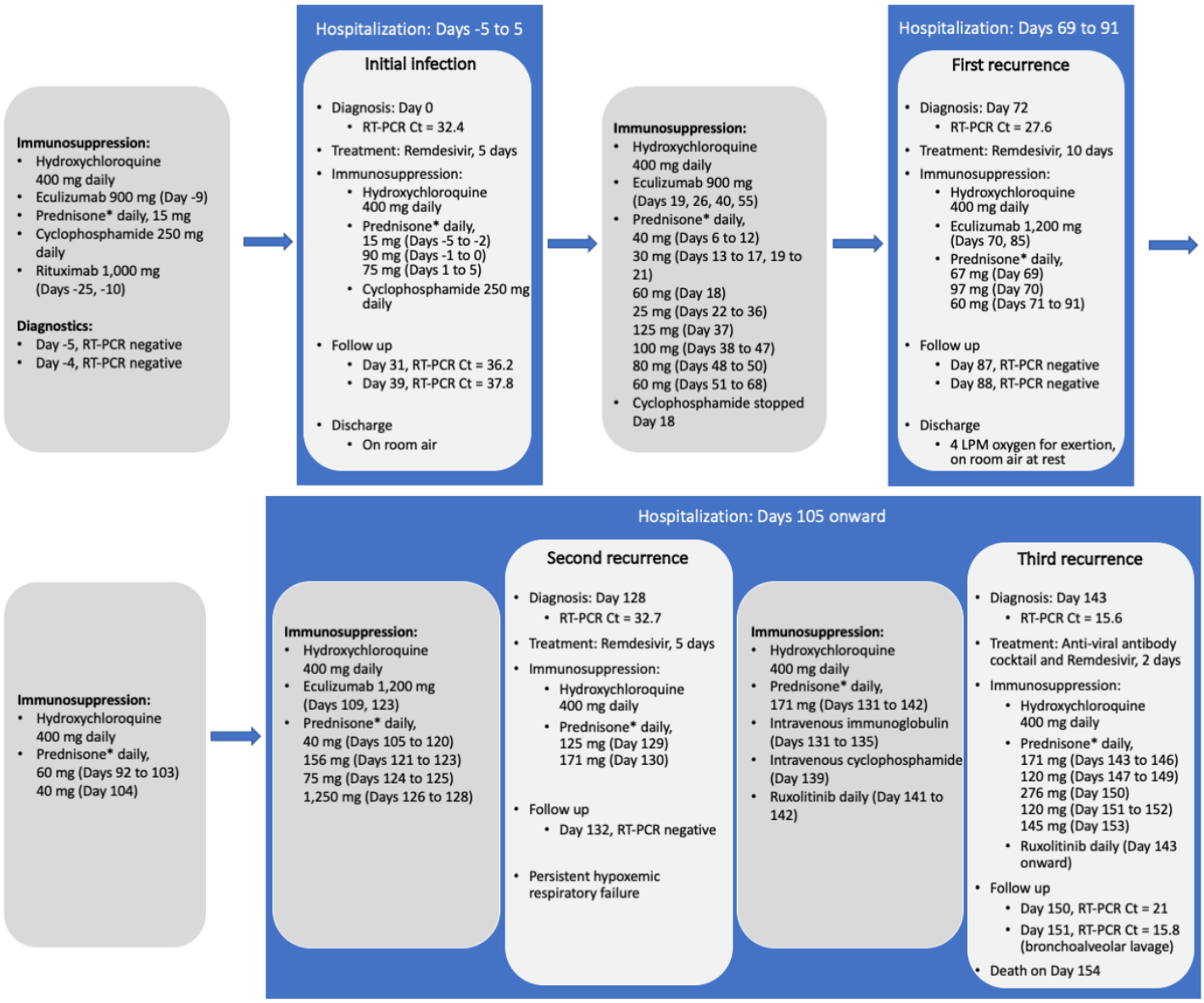

*** Or equivalent daily dose of methylprednisolone, dexamethasone, or combination**

Figure S2: Levels of SARS-CoV-2 viral RNA and time course of immunosuppressive and antiviral treatments. *Top panel:* Nasopharyngeal and bronchoalveolar lavage SARS-CoV-2 RT-PCR cycle threshold (Ct) values (dashed line represents cutoff for positivity at 40) and SARS-CoV-2 antibody testing. Day 0 represents day of first positive SARS-CoV-2 nasopharyngeal swab RT-PCR. Prior nasopharyngeal swab RT-PCR from Days -5 and -4 were negative. *Middle panel:* SARS-CoV-2 RNA viral loads in nasopharyngeal, plasma, and sputum by quantitative RT-PCR assay. Viral load not obtained on Day 132, the day of negative RT-PCR before third recurrence. *Bottom panel:* Immunosuppressive and antiviral treatments.

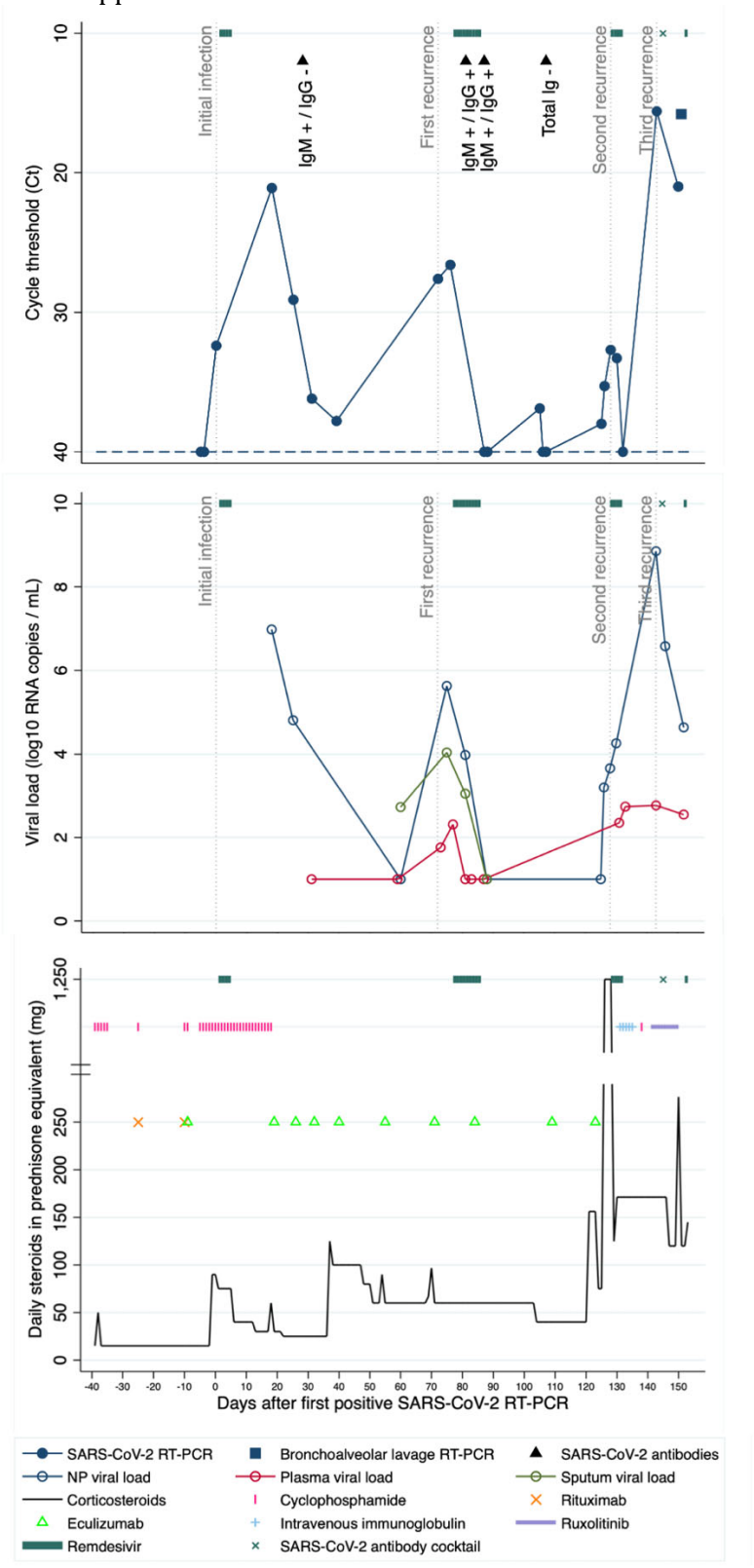

Figure S3: Representative computed tomography (CT) chest images at the level of the right lower lobe bronchus. (A) Day -38. CT without contrast obtained 38 days prior to initial positive RT-PCR swab. (B) Day -1. CT pulmonary angiogram obtained 1 day prior to first positive RT-PCR swab diagnosing Covid-19. Notable for multifocal patchy groundglass opacities with peribronchial distribution and subpleural sparing. Negative for pulmonary embolism. (C) Day 76. CT pulmonary angiogram obtained 4 days after diagnosis of first recurrence of Covid-19. Notable for new peribronchial and subpleural GGOs, reticulation admixed with consolidation and architectural distortion, mild traction bronchiectasis. Negative for pulmonary embolism. (D) Day 111. CT pulmonary angiogram obtained during admission for cellulitis, on day of escalating oxygen requirement. This was 15 days before diagnosis of second recurrence of Covid-19. Notable for worse bilateral patchy GGO and solid opacities. Negative for pulmonary embolism. (E) Day 124. CT pulmonary angiogram obtained due to worsening hypoxemia. This was 2 days before diagnosis of second recurrence of Covid-19. Notable for extensive bilateral GGO with patchy areas of lobular and subpleural sparing, worsening diffuse lung disease with evidence of organization. Negative for pulmonary embolism.

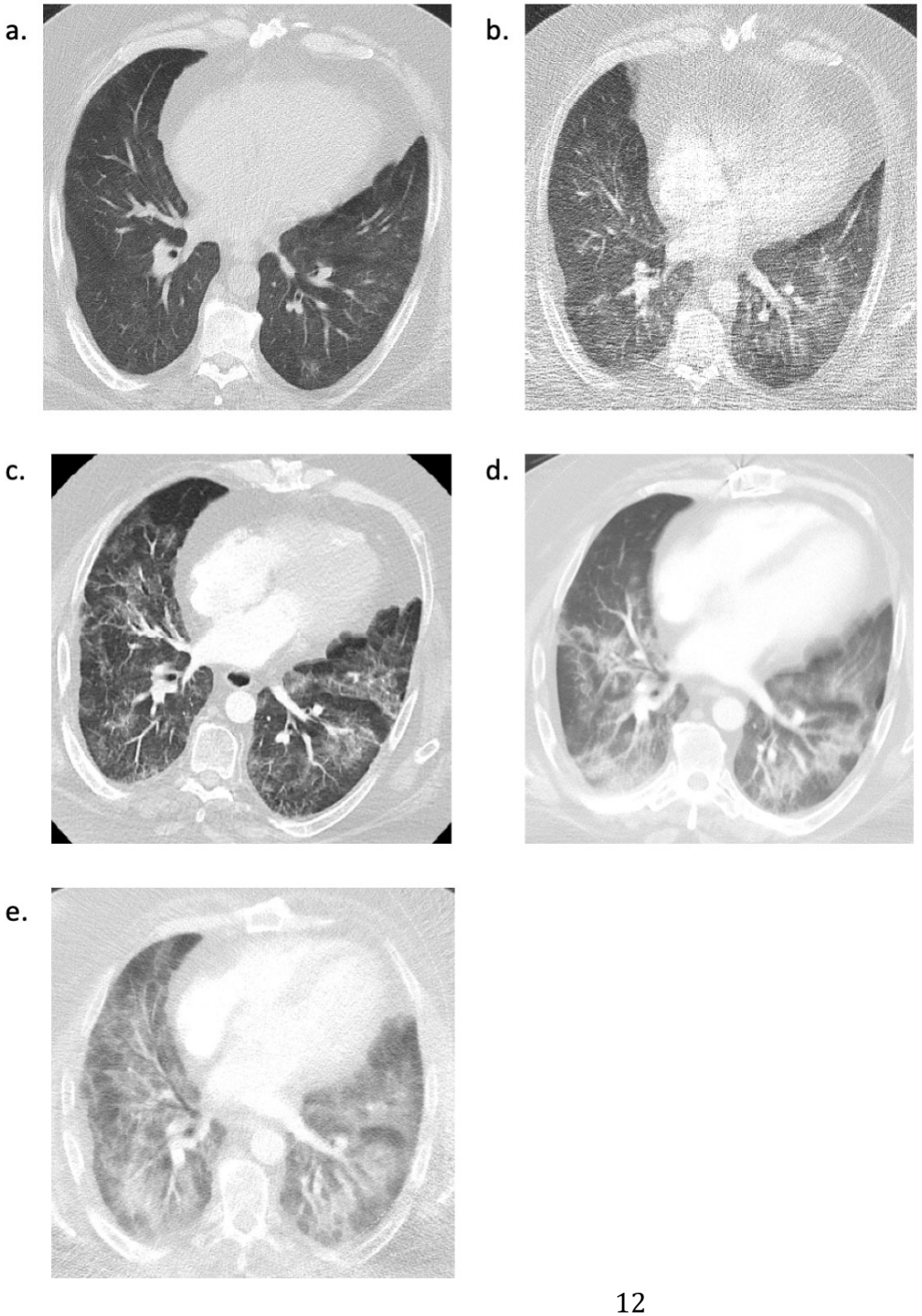

Figure S4: SARS-CoV-2 RNA viral loads and total viral burden from post-mortem exam, by tissue type.

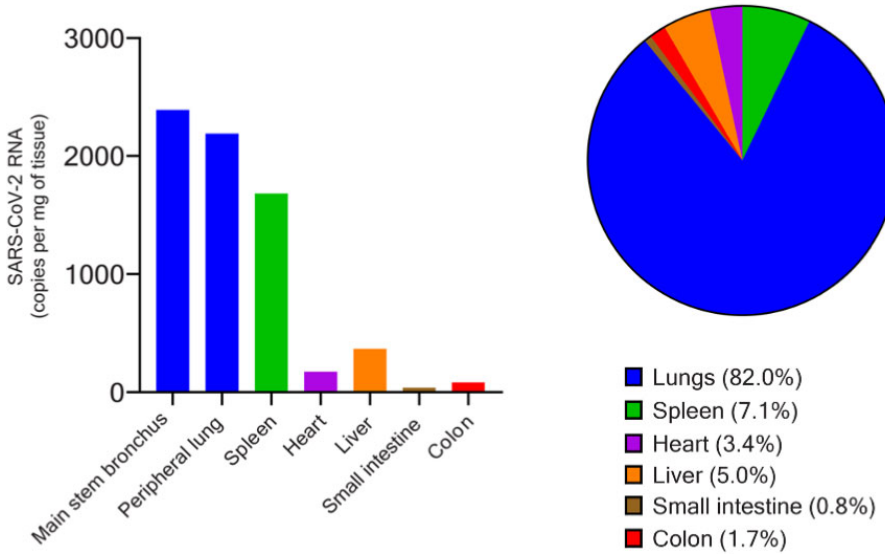

Figure S5: Gross exam and histology from autopsy. *Top left:* Gross photograph of left lung at autopsy showing diffuse alveolar hemorrhage and necrotizing *Aspergillus* pneumonia including a left upper lobe cavitary nodule (arrow). *Top right:* Diffuse alveolar hemorrhage with fresh blood in alveolar spaces as well as abundant hemosiderin-laden macrophages (arrows) indicative of prior episodes. Hematoxylin and eosin (H&E) stained section, 100x original magnification. *Bottom left:* Lymph node with extensive depletion of lymphoid cells including absence of germinal centers. H&E stained section, 20x original magnification. *Bottom right:* Necrotizing *Aspergillus* pneumonia with abundant organisms (arrows). H&E stained section, 200x original magnification.

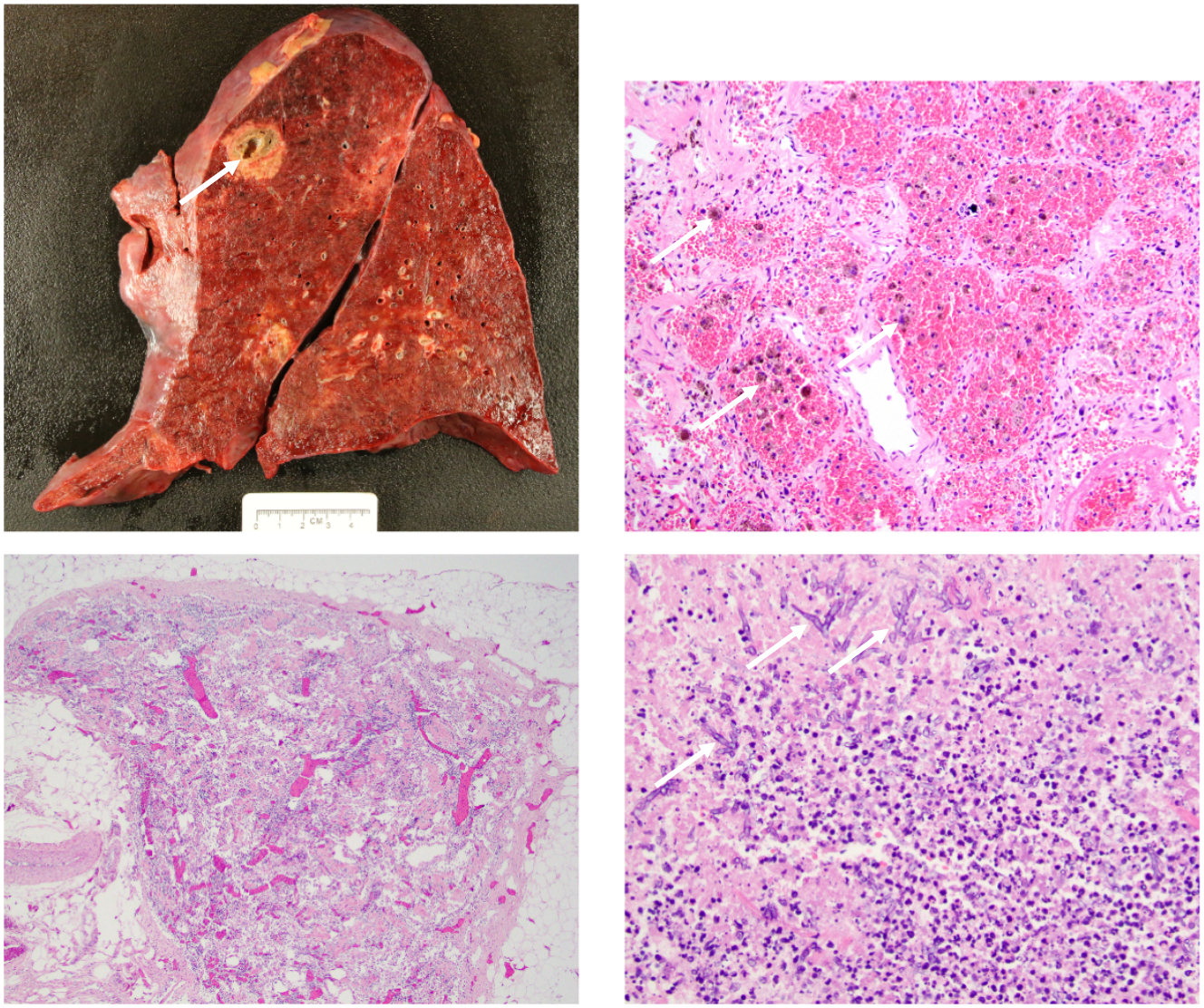

Figure S6: Maximum likelihood phylogenetic tree with patient sequences (red) at three time points, T0 (Day 18, 25), T1 (Day 75, 81), T2 (Day 128, 130), and T3 (Days 143, 146, 152) compared to representative sequences from the state (Massachusetts) and region (Other New England Area).

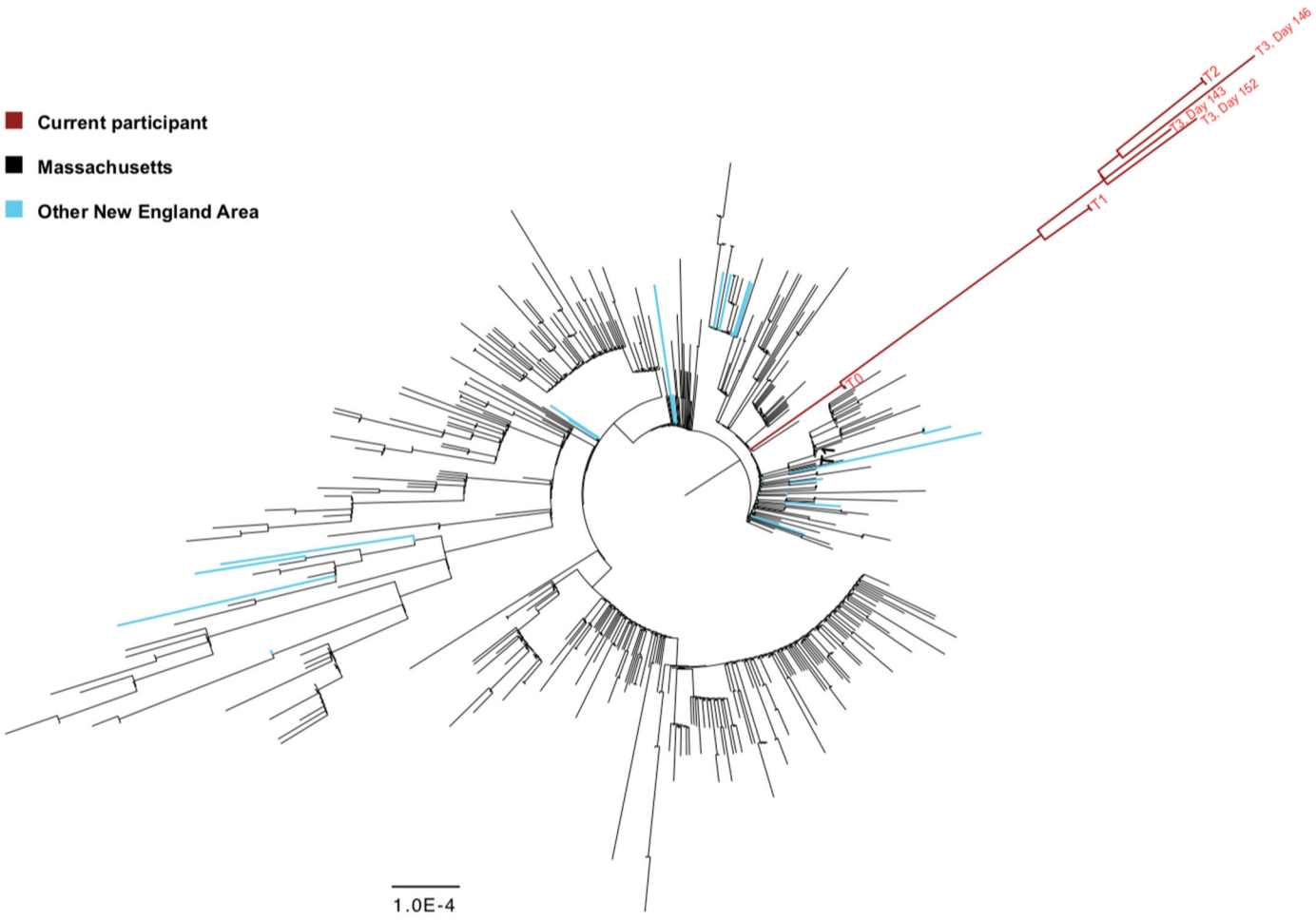

Figure S7: Viral infectivity studies. Epithelial cells (Vero-E6) incubated with nasopharyngeal samples from Days 75 and 143 shown at 96 hours post-infection (hpi), demonstrating SARS-CoV-2 cytopathic effects (CPE) and disrupted cell monolayer. 4x magnification. *Top left:* negative control, no virus, with intact monolayer. *Top right:* positive control, USA-WA1/2020, with disrupted monolayer. *Bottom left:* Day 75 sample, with disrupted monolayer. *Bottom right:* Day 143 sample, CPE and disrupted monolayer.

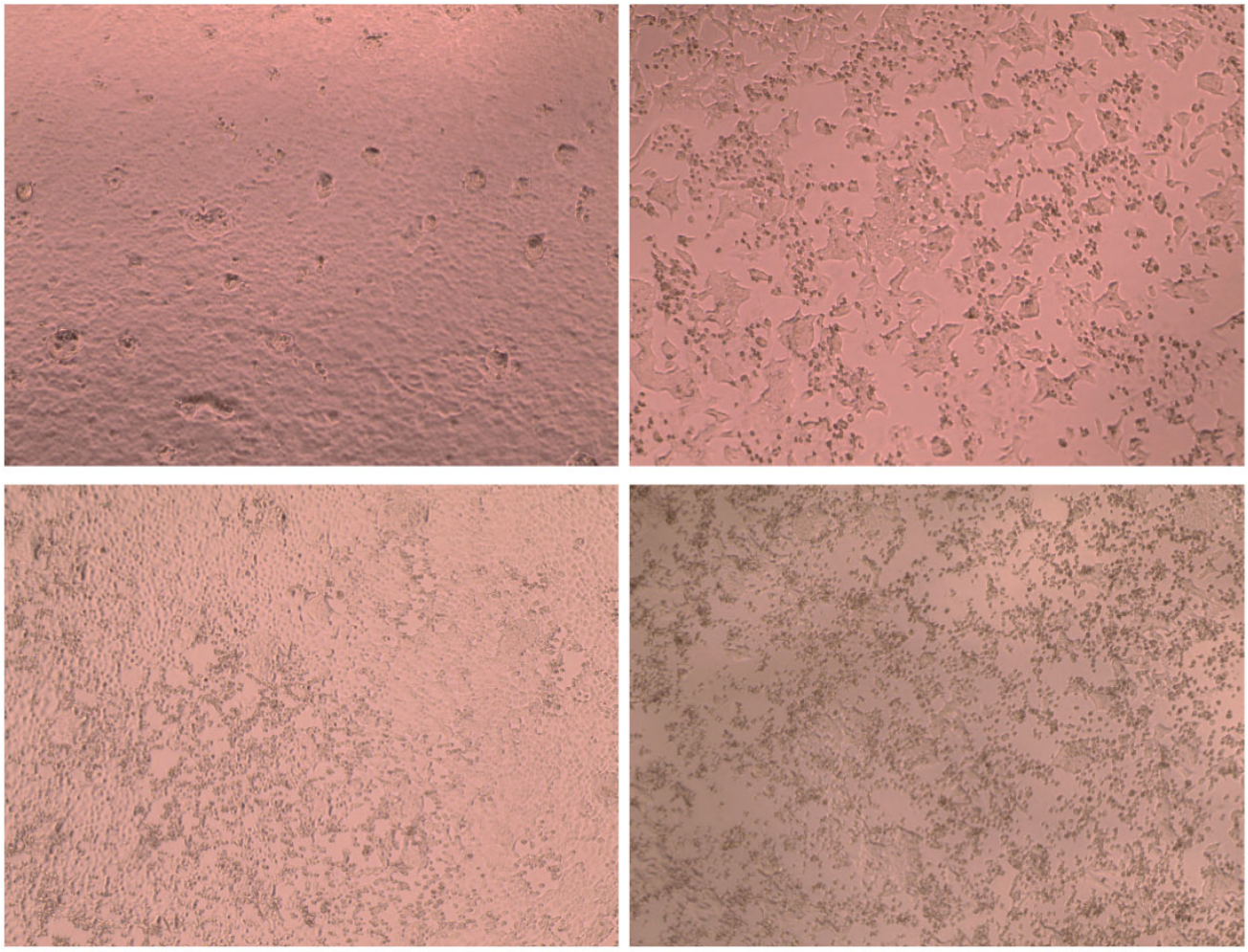

Figure S8: Cell surface immune phenotyping by flow cytometry. Dot plots demonstrate the proportion of circulating immune cell types of age-matched hospitalized patients with active Covid-19 (n=12). Demographic information of the controls in Table S4. Each dot represents an individual patient; this patient labeled in red. Data presented with median and 95% confidence intervals. mDC = myeloid dendritic cells, pDC = plasmacytoid dendritic cells, NK = natural killer, Ab-scrt = antibody-secreting B cells, Non-Ab-scrt = non-antibody-secreting B cells, SM = switched memory, DN = IgD-CD27 Double negative, USM = unswitched memory, NK = natural killer, pos = positive, neg = negative, brt = bright, PD1 = programmed cell death protein 1, Treg = regulatory T cell, Tcm= central memory T cell, Tem = effector memory T cell, Temra = terminally differentiated effector T cell, Tfh = T follicular helper cell, Th17 = T helper 17.

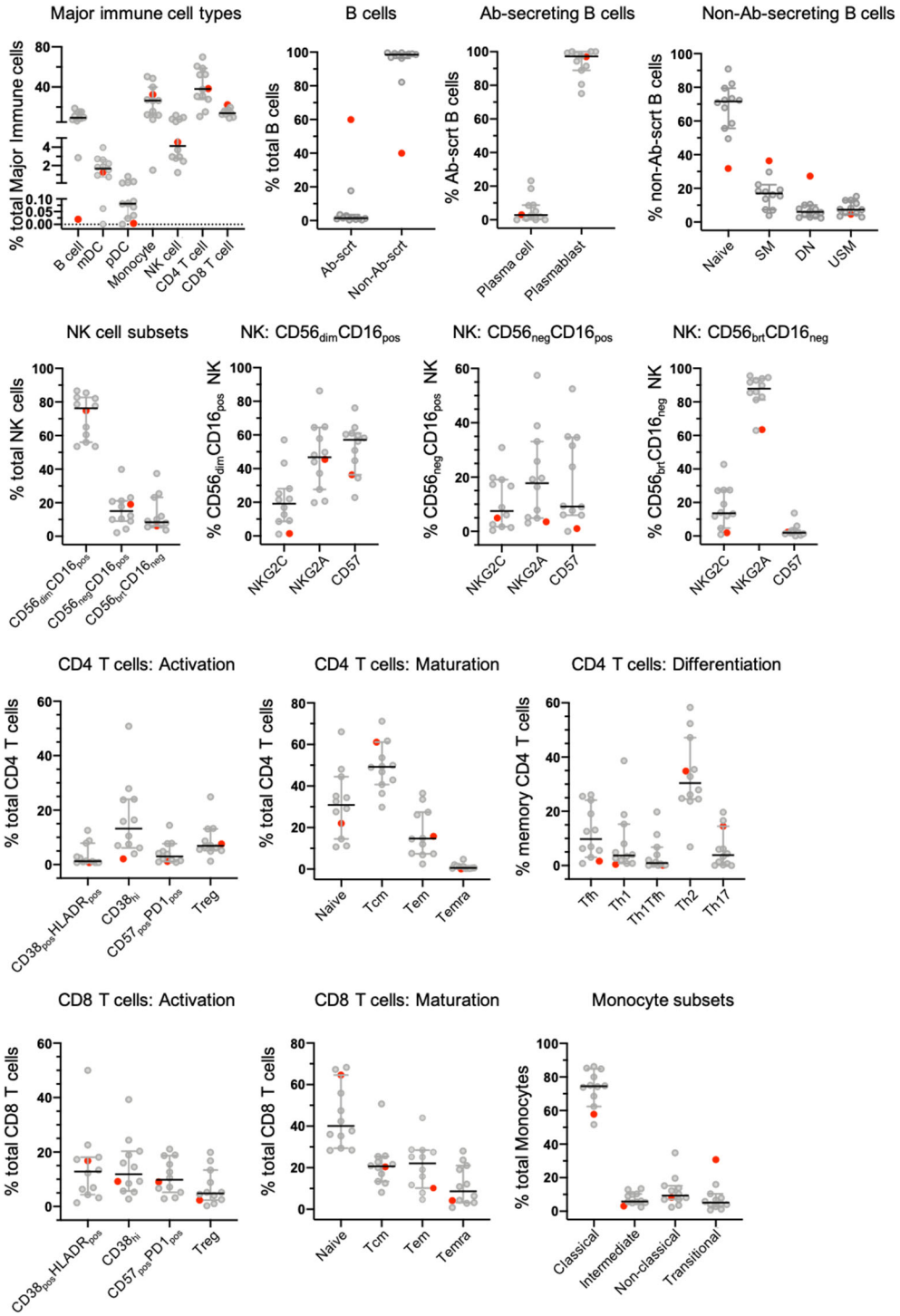

Figure S9: SARS-CoV-2-specific CD4 and CD8 T cell proliferation assay. CSFE (carboxyfluorescein diacetate succinimidyl ester) proliferation in response to cytomegalovirus (CMV) and SARS-CoV-2 peptide pools. NSP = non-structural proteins, NC = nucleocapsid, M = membrane, E = envelope, 3a = Open reading frame 3A.

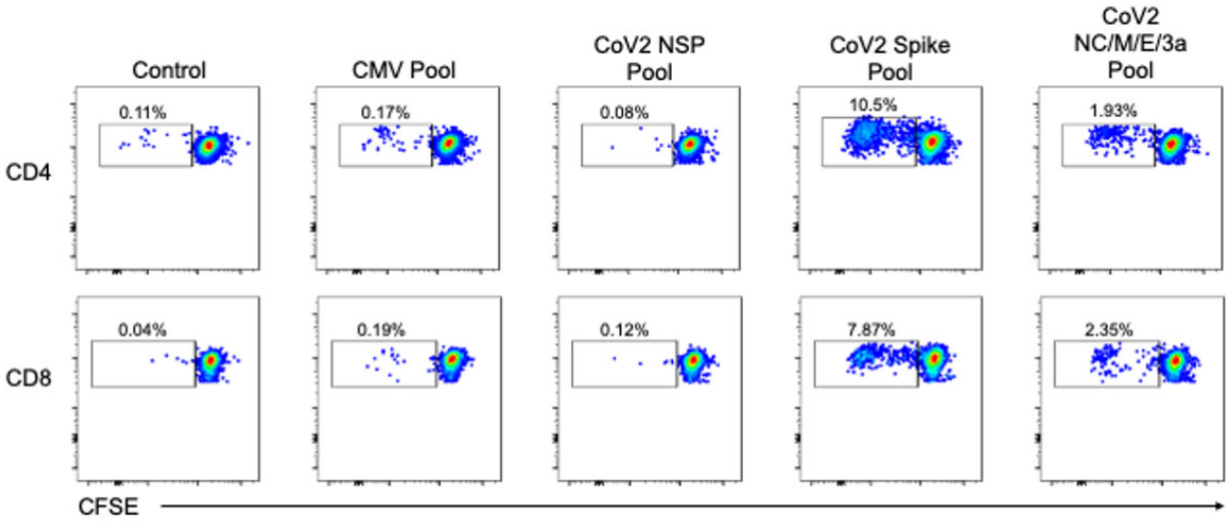

Figure S10: Longitudinal serum SARS-CoV-2 antigen-specific antibody isotypes and subclasses (IgG1, IgA1, and IgM) specific for the SARS-CoV-2 spike protein (S), receptor binding domain (RBD), and nucleocapsid protein (N) at timepoints Days 31 – 152 (Days 31, 59, 73, 77, 81, 83, 87, 131, 133, 146, and 152). Antibody titer specific for recombinant HA-tagged Ebolavirus glycoprotein is shown as a negative control. PE median fluorescent intensity (MFI) was the reported readout for relative antibody titers.

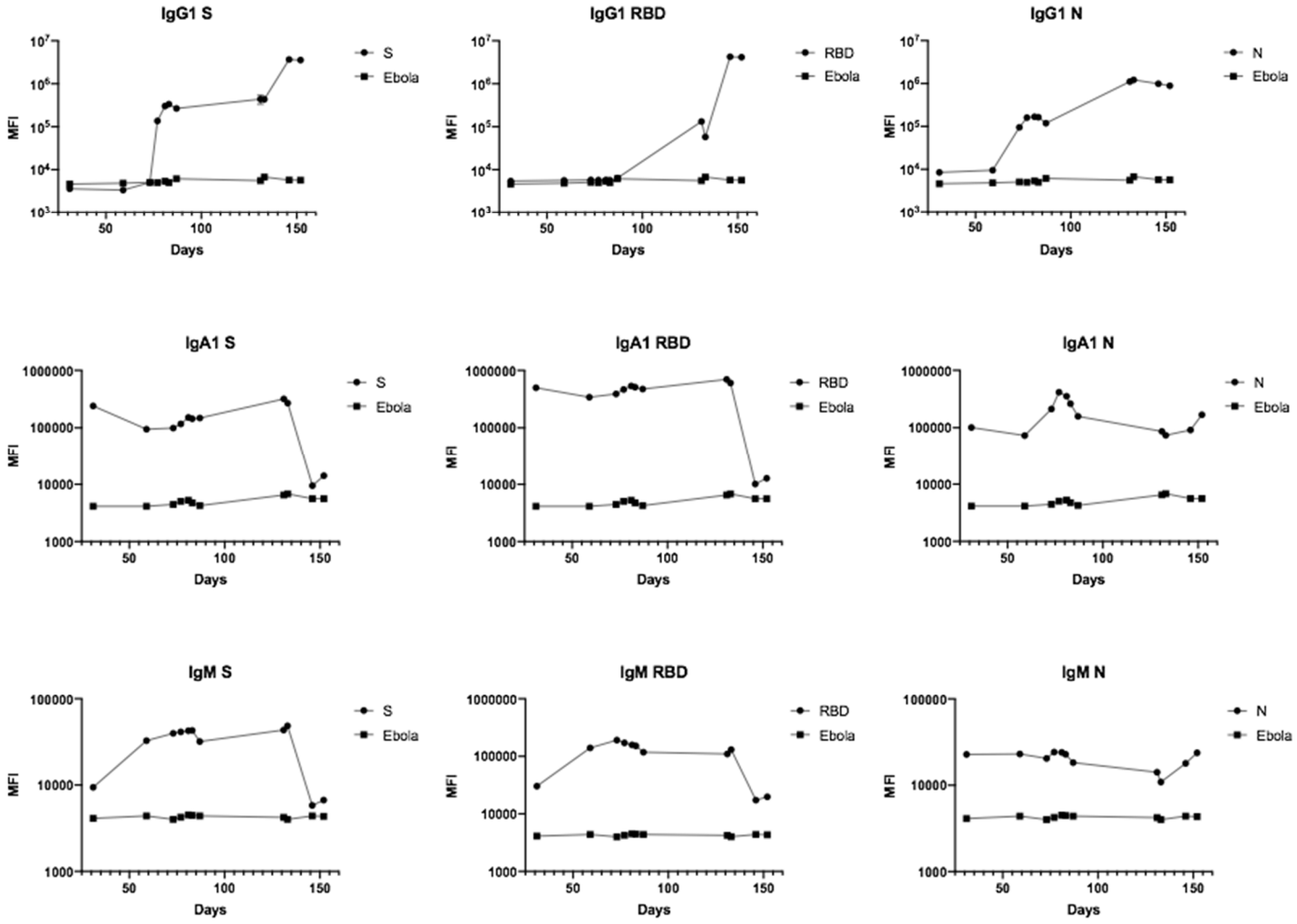

Figure S11: Longitudinal serum neutralizing antibody assay at timepoints between Days 31 to 87. Serum inhibitory dilutions at 50% (ID_{50}) and 80% (ID_{80}) neutralization were attained. Dotted line represents ID_{50}. *Top panel:* Using VRC7480-G614 full length spike from SARS-CoV-2 pseudovirus and 293T/ACE2 target cells. *Bottom panel:* Using deltaCT-D614 truncated spike from SARS-CoV-2 pseudovirus and TZM.bl/ACE2 target cells. NHS = normal human serum (negative control), Positive Pool Serum = pooled Covid-19 convalescent serum (positive control).

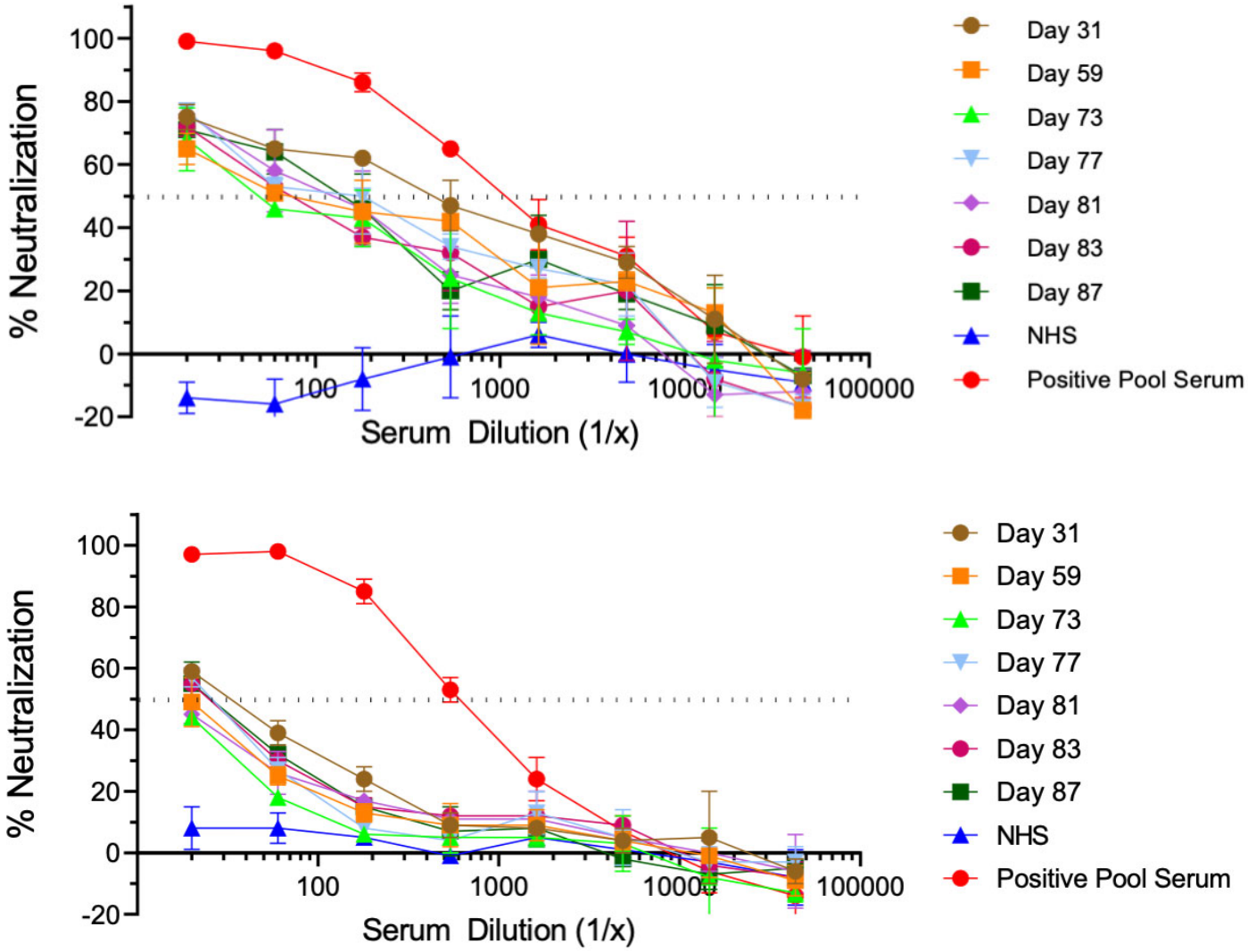

Figure S12: Laboratory values over time, Days -40 to 154.
a) Absolute lymphocyte count, b) Lactate dehydrogenase, c) D-dimer, d) C-reactive protein, e) Ferritin, f) Troponin T-hs Gen5

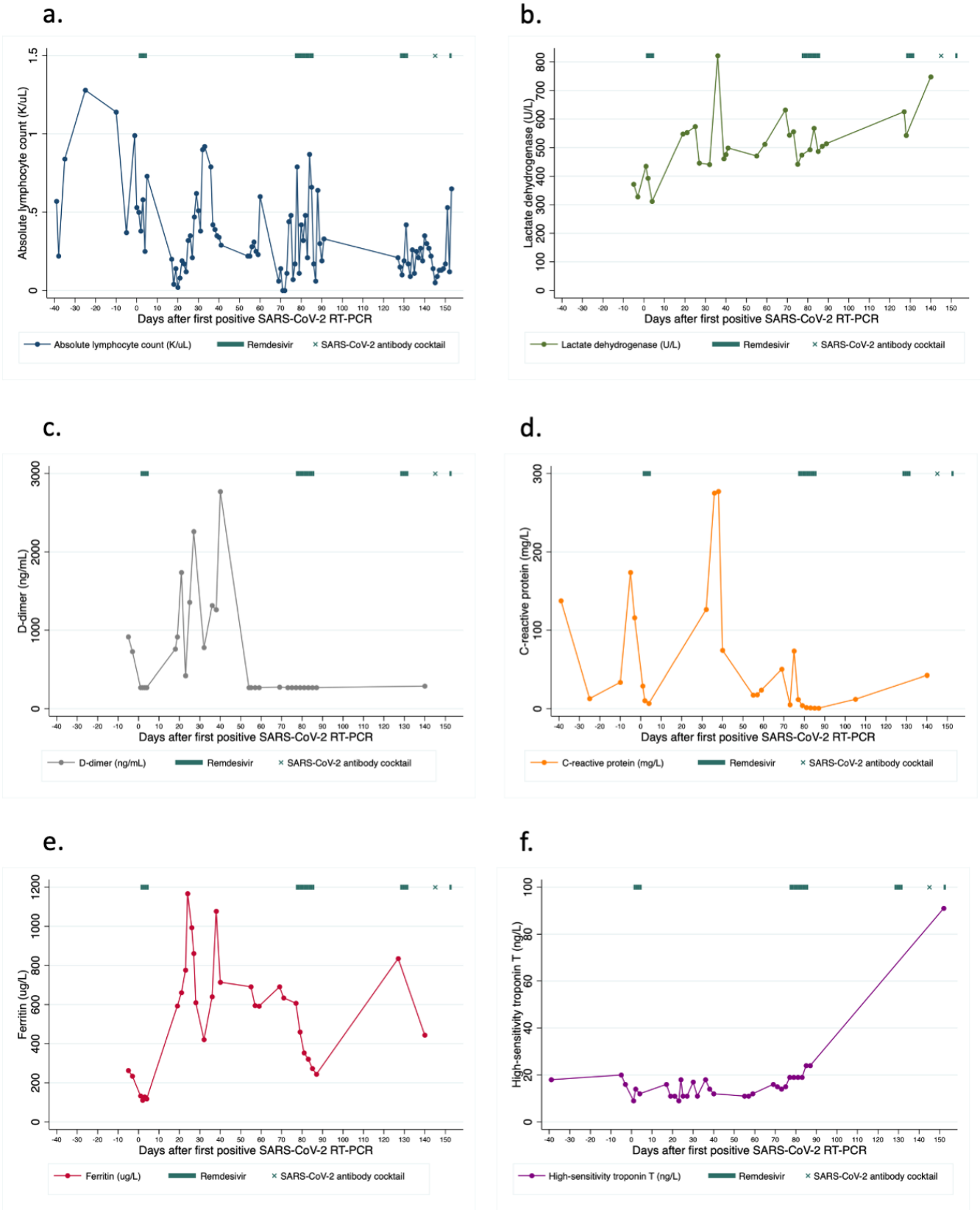

SUPPLEMENTAL TABLES

Table S1: SARS-CoV-2 RT-PCR Ct and quantitative viral load

Day	SARS-CoV-2 RT-PCR Ct	Site	Nasopharyngeal viral load (log_{10} RNA copies/mL)	Plasma viral load (log_{10} RNA copies/mL)	Sputum viral load (log_{10} RNA copies/mL)
-5	Negative	NP			
-4	Negative	NP			
0	32.4	NP			
18	21.2	NP	6.98		
25	29.1	NP	4.81		
31	36.2	NP		1	
36	Positive (Ct not reported)	NP			
39	37.8	NP			
54					
59				1	
60			1		2.73
62					
72	27.6	NP			
73				1.76	
75			5.63		4.04
76	26.6	NP			
77				2.31	
81			3.98	1	3.05
83				1	
87	Negative	NP		1	
88	Negative	NP	1		1
105	36.9	NP			
106	Negative	NP			
107	Negative	NP			
125	38	NP	1		
126	35.3	NP	3.20		
128	32.7	NP	3.66		
130	33.3	NP	4.26		
131				2.35	
132	Negative	NP			
133				2.74	
143	15.6	NP	8.86		
146			6.58	2.77	
150	21	NP			
151	15.8	BAL			
152			4.64	2.55	

BAL = bronchoalveolar lavage, Ct = cycle threshold, NP = nasopharyngeal, RT-PCR = reverse-transcriptase polymerase-chain-reaction

Table S2: Quantitative SARS-CoV2-specific antibody testing

Day	Assay	IgM	IgG	Target antigen
28	Epitope Diagnostics EDI Novel Coronavirus COVID-19 Enzyme Linked Immunosorbent Assay (ELISA)	1.734 (cutoff >0.731)	0.350, negative (cutoff >0.955)	Recombinant nucleocapsid protein (N)
81	Epitope Diagnostics EDI Novel Coronavirus COVID-19 Enzyme Linked Immunosorbent Assay (ELISA)	1.444 (cutoff >0.999)	1.917 (cutoff >0.999)	Recombinant nucleocapsid protein (N)
87	Epitope Diagnostics EDI Novel Coronavirus COVID-19 Enzyme Linked Immunosorbent Assay (ELISA)	1.049 (cutoff >0.999)	1.414 (cutoff >0.999)	Recombinant nucleocapsid protein (N)
Day	**Assay**	**Antibody index**		
107	Roche Elecsys assay of total immunoglobulins (IgM, IgG, and IgA)	0.1 (cutoff >1.0)		Recombinant nucleocapsid protein (N)

Table S3: Resistance mutation profile of different time-point samples of current participant against REGN10933 and REGN10987. Mutations against REGN10933 are highlighted in black, against REGN10987 highlighted in red and against both REGN10987+REGN10933 are highlighted with red, bold, underlined. Sequences with a mutation in that cell is denoted by "x" while polymorphism is written out in the cell.

	K417E	K444Q	V445A	Y453F	L455F	F486V	Q493K	H655Y	R682Q	R685S	V687G	G769E
T0, Day 18												
T0, Day 25												
T1, Day 75												
T1, Day 81												
T2, Day 128							x					
T2, Day 130							x					
T3, Day 143												
T3, Day 146							x					
T3, Day 152						486I						

Table S4: Demographic information for the age-matched hospitalized controls with active Covid-19 (n=11) in immune phenotyping by flow cytometry, as shown in Figure S8.

Gender (M=Male, F=Female)	Race	Ethnicity	Age	Sample Date (Days since first + SARS-CoV-2 RT-PCR)	Intubated	ICU care	Deceased	Prior immunotherapy	Corticosteroids	Corticosteroid dosing	Biologics
M	Unknown	Hispanic/ Latino	44	11*	Y	Y	N	No	Yes	Dexamethasone (8-16mg) on Day -1 and Day 11	No
M	White	Not Hispanic or Latino	54	39	Y	Y	N	No	No	none	No
M	Unknown	Hispanic/ Latino	46	19	Y	Y	Y	No	Yes	Dexamethasone Days 4-13 (10-20mg)	Tocilizumab (Day 0)
M	Unknown	Not Hispanic or Latino	57	17	Y	Y	N	No	Yes	Methylprednisolone 40mg (Day 16); home fluticasone	No
F	White	Not Hispanic or Latino	43	16	Y	Y	N	No	No	Home fluticasone	No
F	Black/ African American	Not Hispanic or Latino	47	8	N	N	N	No	Yes	Prednisone 50mg (Day 7); home fluticasone	Tocilizumab (Day 7)
M	White	Not Hispanic or Latino	60	14	Y	Y	N	No	Yes	Hydrocortisone 50-200 mg (Days 5-7); methylprednisolone 20 mg (Days 7-8); prednisone 20 mg (Days 8-14)	No
F	Unknown	Unknown	43	41	Y	Y	N	No	No	Home fluticasone/salmeterol inhaler	No
F	Unknown	Hispanic/ Latino	60	33	Y	Y	Y	No	No	none	Sarilumab (Day 0)
M	Asian	Not Hispanic or Latino	47	61	Y	Y	N	No	Yes	Hydrocortisone 100-150mg (Days 13-14); home fluticasone and mometasone	Anakinra (Days 8-10)
F	Black/ African American	Not Hispanic or Latino	41	12	Y	Y	N	No	Yes	Methylprednisolone 40mg (Day 0)	No

*May have tested positive days prior at different hospital.

RT-PCR = reverse transcription polymerase chain reaction

Table S5: Vital signs and laboratory data (day of ± 3 days)

	Day 0 (Initial infection)	**Day 72 (First recurrence)**	**Day 128 (Second recurrence)**	**Day 143 (Third recurrence)**
Vital signs				
Maximum temperature (°Celsius) and mode	36.4 oral	36.7 oral	37 oral	36.9 oral
Heart rate	74 to 78	68 to 94	74 to 92	86 to 107
Cuff blood pressure (mmHg)	130/68 to 148/92	121/67 to 166/65	94/65 to 126/89	98/70 to 129/80
Respiratory rate (breaths/minute)	18 to 20	19 to 22	17 to 35	19 to 46
SpO2 (%)	92 to 93	92 to 98	89 to 97	87 to 97
O2 amount and device required at rest	None	3.5 LPM NC	60% to 80%, 60 LPM HFNC	75% to 90%, 60 LPM HFNC
Laboratory data				
Total white blood cell count (K/uL)	7.11	5.68	9.18	8.61
Lymphocyte count (K/uL)	0.53	0.00	0.15	0.22
Platelet count (K/uL)	205	74	158	143
Hemoglobin (g/dL)	8.8	10.0	10.5	11.5
Lactate dehydrogenase (U/L)	435	556	543	748
D-dimer (ng/mL)	<270	<270	-	289
C-reactive protein (mg/L)	29.0	5.1	-	42.6
Serum ferritin (µg/L)	133	634	835	444
High-sensitivity troponin T (ng/L)	9	14	-	-
IL-6 (pg/mL)	-	-	-	7.0

HFNC = high flow nasal cannula, LPM = liters per minute, NC = nasal cannula

Table S6: GISAID (https://www.gisaid.org) accession numbers

GISAID Accession Number	Viral Name	Collection Date
EPI_ISL_418241	hCoV-19/Algeria/G0638_2264/2020	3/2/20
EPI_ISL_420598	hCoV-19/Argentina/C3013/2020	3/22/20
EPI_ISL_419693	hCoV-19/Belarus/ChVir2073/2020	2020-03
EPI_ISL_414016	hCoV-19/Brazil/SPBR-05/2020	2/29/20
EPI_ISL_414477	hCoV-19/Czech Republic/951/2020	3/1/20
EPI_ISL_416141	hCoV-19/Denmark/SSI-09/2020	3/3/20
EPI_ISL_417418	hCoV-19/Italy/FVG-ICGEB_S1/2020	3/1/20
EPI_ISL_416479	hCoV-19/Georgia/Tb-273/2020	3/5/20
EPI_ISL_416741	hCoV-19/Lithuania/ChVir1632/2020	2020-02
EPI_ISL_414027	hCoV-19/Scotland/CVR05/2020	3/4/20
EPI_ISL_417877	hCoV-19/Slovakia/SK-BMC1/2020	3/6/20
EPI_ISL_419562	hCoV-19/Luxembourg/LNS0000001/2020	2/29/20
EPI_ISL_416756	hCoV-19/France/Lyon_06531/2020	3/6/20
EPI_ISL_417536	hCoV-19/Iceland/10/2020	3/16/20
EPI_ISL_420795	hCoV-19/USA/RI_0556/2020	3/1/20
EPI_ISL_419553	hCoV-19/USA/RI_0520/2020	2/28/20
EPI_ISL_418251	hCoV-19/Spain/Madrid201105/2020	2/25/20
EPI_ISL_418981	hCoV-19/Belgium/VRAR-030643/2020	3/6/20
EPI_ISL_418420	hCoV-19/France/ARA10170/2020	3/17/20
EPI_ISL_418206	hCoV-19/Senegal/003/2020	2/28/20
EPI_ISL_420791	hCoV-19/USA/NH_0004/2020	2/29/20
EPI_ISL_421560	hCoV-19/USA/UT-00035/2020	3/18/20
EPI_ISL_424887	hCoV-19/USA/RI_0702/2020	3/5/20
EPI_ISL_426435	hCoV-19/USA/RI_0882/2020	3/9/20
EPI_ISL_416745	hCoV-19/France/Pollionay_1733/2020	3/10/20
EPI_ISL_416489	hCoV-19/USA/WI-02/2020	3/15/20
EPI_ISL_421653	hCoV-19/Latvia/0001/2020	3/25/20
EPI_ISL_417948	hCoV-19/Congo/108/2020	3/19/20
EPI_ISL_421584	hCoV-19/USA/NJ-NYUMC83/2020	3/18/20
EPI_ISL_421389	hCoV-19/USA/NY-PV08434/2020	3/18/20
EPI_ISL_418973	hCoV-19/USA/NY-NYUMC27/2020	3/17/20
EPI_ISL_420205	hCoV-19/England/SHEF-C034F/2020	3/29/20
EPI_ISL_420350	hCoV-19/Belgium/BDW-030694/2020	3/6/20
EPI_ISL_418813	hCoV-19/Canada/MB_10/2020	3/13/20
EPI_ISL_415129	hCoV-19/England/20099038206/2020	2/29/20
EPI_ISL_412972	hCoV-19/Mexico/CDMX-InDRE_01/2020	2/27/20
EPI_ISL_416428	hCoV-19/Vietnam/39607/2020	3/7/20
EPI_ISL_416430	hCoV-19/Vietnam/CM295/2020	3/6/20
EPI_ISL_420568	hCoV-19/Italy/6193/2020	3/23/20
EPI_ISL_412912	hCoV-19/Germany/Baden-Wuerttemberg-1/2020	2/25/20
EPI_ISL_419210	hCoV-19/Israel/ISR_IT0320/2020	2020-03
EPI_ISL_421684	hCoV-19/USA/MN128-MDH128/2020	3/16/20
EPI_ISL_420065	hCoV-19/Estonia/ChVir1982/2020	2020-03
EPI_ISL_418263	hCoV-19/Greece/10/2020	3/18/20
EPI_ISL_415787	hCoV-19/Peru/010/2020	3/10/20

EPI_ISL_420899	hCoV-19/Germany/BAV-V2010492/2020	3/11/20
EPI_ISL_418250	hCoV-19/Spain/Cataluna201396/2020	2020
EPI_ISL_417571	hCoV-19/Iceland/243/2020	3/17/20
EPI_ISL_421651	hCoV-19/Taiwan/225/2020	3/22/20
EPI_ISL_420153	hCoV-19/Norway/2090/2020	3/16/20
EPI_ISL_413020	hCoV-19/Switzerland/1000477377/2020	2/27/20
EPI_ISL_421275	hCoV-19/Russia/Moscow_PMVL-1/2020	3/18/20
EPI_ISL_413556	hCoV-19/Wales/PHW2/2020	3/4/20
EPI_ISL_418184	hCoV-19/USA/WI-GMF-00018/2020	3/18/20
EPI_ISL_419654	hCoV-19/Austria/CeMM0001/2020	3/3/20
EPI_ISL_416488	hCoV-19/Poland/PL_P1/2020	3/3/20
EPI_ISL_411902	hCoV-19/Cambodia/0012/2020	1/27/20
EPI_ISL_407079	hCoV-19/Finland/1/2020	1/29/20
EPI_ISL_403962	hCoV-19/Nonthaburi/61/2020	1/8/20
EPI_ISL_413618	hCoV-19/USA/CruiseA-13/2020	2/20/20
EPI_ISL_402125	hCoV-19/Wuhan-Hu-1/2019	12/31/19
EPI_ISL_410301	hCoV-19/Nepal/61/2020	1/13/20
EPI_ISL_413617	hCoV-19/USA/CruiseA-12/2020	2/20/20
EPI_ISL_413609	hCoV-19/USA/CruiseA-4/2020	2/21/20
EPI_ISL_410719	hCoV-19/Singapore/11/2020	2/2/20
EPI_ISL_419211	hCoV-19/Israel/ISR_JP0320/2020	2020-03
EPI_ISL_420889	hCoV-19/Japan/Hu_DP_Kng_19-031/2020	2/14/20
EPI_ISL_413619	hCoV-19/USA/CruiseA-14/2020	2/25/20
EPI_ISL_419561	hCoV-19/USA/TX_2020/2020	2/29/20
EPI_ISL_421466	hCoV-19/Portugal/PT0063/2020	3/20/20
EPI_ISL_418379	hCoV-19/Canada/ON_PHL7512/2020	3/13/20
EPI_ISL_413606	hCoV-19/USA/CruiseA-1/2020	2/17/20
EPI_ISL_413851	hCoV-19/Guangdong/2020XN4373-P0039/2020	1/30/20
EPI_ISL_415461	hCoV-19/Netherlands/Gelderland_1/2020	3/10/20
EPI_ISL_416696	hCoV-19/USA/WA-UW158/2020	3/13/20
EPI_ISL_417514	hCoV-19/USA/WI-22/2020	3/13/20
EPI_ISL_415128	hCoV-19/Brazil/ES-225/2020	2/29/20
EPI_ISL_418582	hCoV-19/Ireland/22901/2020	3/10/20
EPI_ISL_419566	hCoV-19/Luxembourg/LNS0641910/2020	3/5/20
EPI_ISL_417483	hCoV-19/Norway/1379/2020	2/27/20
EPI_ISL_419675	hCoV-19/Spain/Valencia11/2020	3/20/20
EPI_ISL_420541	hCoV-19/Slovenia/808/2020	3/5/20
EPI_ISL_418243	hCoV-19/Spain/Andalucia201272/2020	2/28/20
EPI_ISL_419425	hCoV-19/Wales/PHWC-24534/2020	3/18/20
EPI_ISL_420799	hCoV-19/Korea/BA-ACH_2604/2020	2/27/20
EPI_ISL_420800	hCoV-19/Korea/BA-ACH_2718/2020	2/29/20
EPI_ISL_416605	hCoV-19/Japan/DP0481/2020	2/16/20
EPI_ISL_413557	hCoV-19/USA/CA-CDPH-UC1/2020	2/28/20
EPI_ISL_417175	hCoV-19/USA/WA-S122/2020	3/2/20
EPI_ISL_416466	hCoV-19/USA/WA-S11/2020	3/3/20
EPI_ISL_417163	hCoV-19/USA/WA-S110/2020	3/5/20
EPI_ISL_416709	hCoV-19/USA/WA-UW171/2020	3/13/20

EPI_ISL_421690	hCoV-19/USA/MN134-MDH134/2020	3/16/20
EPI_ISL_413931	hCoV-19/USA/CA-CDPH-UC11/2020	3/5/20
EPI_ISL_413523	hCoV-19/India/1-31/2020	1/31/20
EPI_ISL_414577	hCoV-19/Chile/Talca-1/2020	3/2/20
EPI_ISL_416314	hCoV-19/Hong Kong/CUHK1/2020	2/7/20
EPI_ISL_417444	hCoV-19/Pakistan/Gilgit1/2020	3/4/20
EPI_ISL_415581	hCoV-19/Canada/BC_02421/2020	3/1/20
EPI_ISL_413490	hCoV-19/New Zealand/01/2020	2/27/20
EPI_ISL_417521	hCoV-19/Taiwan/CGMH-CGU-08/2020	3/10/20
EPI_ISL_421262	hCoV-19/Nanchang/JX155/2020	1/29/20
EPI_ISL_414520	hCoV-19/Germany/BavPat2/2020	3/2/20
EPI_ISL_414476	hCoV-19/USA/NY1-PV08001/2020	2/29/20
EPI_ISL_417918	hCoV-19/Malaysia/188407/2020	3/18/20
EPI_ISL_417917	hCoV-19/Malaysia/189332/2020	3/20/20
EPI_ISL_416432	hCoV-19/Saudi Arabia/KAIMRC-Alghoribi/2020	3/7/20
EPI_ISL_416706	hCoV-19/USA/WA-UW168/2020	3/13/20
EPI_ISL_421573	hCoV-19/South Africa/KRISP_0006/2020	3/31/20
EPI_ISL_408484	hCoV-19/Sichuan/IVDC-SC-001/2020	1/15/20
EPI_ISL_420024	hCoV-19/USA/VA-DCLS-0043/2020	3/27/20
EPI_ISL_420025	hCoV-19/USA/VA-DCLS-0044/2020	3/27/20
EPI_ISL_414483	hCoV-19/USA/CruiseA-24/2020	2/17/20
EPI_ISL_415661	hCoV-19/Chile/Santiago_op4d1/2020	3/8/20
EPI_ISL_415151	hCoV-19/USA/NY2-PV08100/2020	3/4/20
EPI_ISL_419709	hCoV-19/Spain/PaisVasco201602/2020	3/4/20
EPI_ISL_416348	hCoV-19/Shanghai/SH0039/2020	2/6/20
EPI_ISL_418977	hCoV-19/USA/NY-NYUMC31/2020	3/17/20
EPI_ISL_416541	hCoV-19/Kuwait/KU09/2020	3/2/20
EPI_ISL_421662	hCoV-19/India/1073/2020	3/10/20
EPI_ISL_413488	hCoV-19/Germany/NRW-01/2020	2/28/20
EPI_ISL_409067	hCoV-19/USA/MA1/2020	1/29/20
EPI_ISL_427161	hCoV-19/USA/CT-UW-3845/2020	3/25/20
EPI_ISL_411929	hCoV-19/South Korea/SNU01/2020	2020-01
EPI_ISL_460472	hCoV-19/USA/MA-MGH-00005/2020	3/11/20
EPI_ISL_460221	hCoV-19/USA/MA-MGH-00187/2020	3/26/20
EPI_ISL_460333	hCoV-19/USA/MA-MGH-00428/2020	3/6/20
EPI_ISL_460277	hCoV-19/USA/MA-MGH-00716/2020	4/8/20
EPI_ISL_460278	hCoV-19/USA/MA-MGH-00715/2020	4/8/20
EPI_ISL_460097	hCoV-19/USA/MA-MGH-00568/2020	3/22/20
Pending	hCoV-19/USA/MA_Mass_JL17/2020	4/8/20
Pending	hCoV-19/USA/MA_BWH_JL155/2020	4/23/20
Pending	hCoV-19/USA/MA_BWH_JL162/2020	4/25/20
Pending	hCoV-19/USA/MA_BWH_JL149/2020	4/28/20
Pending	hCoV-19/USA/MA_BWH_JL154/2020	4/23/20
Pending	hCoV-19/USA/MA_BWH_JL147/2020	4/23/20
Pending	hCoV-19/USA/MA_BWH_JL150/2020	4/27/20
Pending	hCoV-19/USA/MA_BWH_JL159/2020	4/23/20
Pending	hCoV-19/USA/MA_Mass_JL4/2020	3/26/20

EPI_ISL_593478	hCoV-19/USA/MA_Mass_819_T0_428/2020	4/28/20
EPI_ISL_593479	hCoV-19/USA/MA_Mass_819_T0_55/2020	5/5/20
Pending	hCoV-19/USA/MA_BWH_JL161/2020	4/23/20
Pending	hCoV-19/USA/MA_Mass_JL18S/2020	4/1/20
Pending	hCoV-19/USA/MA_Mass_JL17O/2020	4/8/20
Pending	hCoV-19/USA/MA_Mass_JL17S/2020	4/8/20
Pending	hCoV-19/USA/MA_Mass_JL26N/2020	5/4/20
Pending	hCoV-19/USA/MA_Mass_JL26O/2020	5/4/20
Pending	hCoV-19/USA/MA_Mass_JL26S/2020	5/4/20
Pending	hCoV-19/USA/MA_BWH_JL164/2020	4/25/20
Pending	hCoV-19/USA/MA_BWH_JL166/2020	4/28/20
EPI_ISL_460440	hCoV-19/USA/MA-MGH-00006/2020	3/11/20
EPI_ISL_460318	hCoV-19/USA/MA-MGH-00674/2020	4/5/20
EPI_ISL_460297	hCoV-19/USA/MA-MGH-00064/2020	3/25/20
EPI_ISL_460138	hCoV-19/USA/MA-MGH-00544/2020	3/20/20
EPI_ISL_460098	hCoV-19/USA/MA-MGH-00277/2020	4/1/20
EPI_ISL_460246	hCoV-19/USA/MA-MGH-00717/2020	4/8/20
Pending	hCoV-19/USA/MA_BWH_JL145/2020	4/28/20
EPI_ISL_460455	hCoV-19/USA/MA-MGH-00250/2020	4/6/20
EPI_ISL_460323	hCoV-19/USA/MA-MGH-00721/2020	4/8/20
EPI_ISL_467866	hCoV-19/USA/MA-QDX-80/2020	3/14/20
EPI_ISL_491316	hCoV-19/USA/MA-UW-633/2020	6/27/20
EPI_ISL_491317	hCoV-19/USA/MA-UW-673/2020	6/26/20
EPI_ISL_460130	hCoV-19/USA/MA-MGH-00706/2020	4/7/20
Pending	hCoV-19/USA/MA_Mass_JL22/2020	4/20/20
Pending	hCoV-19/USA/MA_Mass_JL19/2020	4/7/20
Pending	hCoV-19/IND/GBRC268a/2020	7/17/20
Pending	hCoV-19/USA/MA_Mass_JL20/2020	4/15/20
EPI_ISL_593480	hCoV-19/USA/MA_Mass_819_T1_624/2020	6/24/20
EPI_ISL_593553	hCoV-19/USA/MA_Mass_819_T1_630/2020	6/30/20
EPI_ISL_593554	hCoV-19/USA/MA_Mass_819_T2_816/2020	8/16/20
EPI_ISL_593555	hCoV-19/USA/MA_Mass_819_T2_818/2020	8/18/20
EPI_ISL_593556	hCoV-19/USA/MA_Mass_819_T3_831/2020	8/31/20
EPI_ISL_593557	hCoV-19/USA/MA_Mass_819_T3_93/2020	9/3/20
EPI_ISL_593558	hCoV-19/USA/MA_Mass_819_T3_99/2020	9/9/20
EPI_ISL_415152	hCoV-19/Panama/328677/2020	3/6/20
EPI_ISL_424174	hCoV-19/USA/CT-UW-1365/2020	3/13/20

Table S7: NCBI (https://www.ncbi.nlm.nih.gov/nuccore/?term=) accession numbers

Accession Number	Viral Name	Collection Date
MT520172	MA_MGH_00568/2020	3/22/20
MT520173	MA_MGH_00277/2020	4/1/20
MT520175	MA_MGH_00278/2020	4/1/20
MT520176	MA_MGH_00016/2020	3/25/20
MT520177	MA_MGH_00018/2020	3/25/20
MT520178	MA_MGH_00426/2020	3/7/20
MT520179	MA_MGH_00050/2020	3/24/20
MT520180	MA_MGH_00042/2020	3/25/20
MT520182	MA_MGH_00157/2020	3/26/20
MT520183	MA_MGH_00208/2020	3/27/20
MT520185	MA_MGH_00485/2020	3/27/20
MT520186	MA_MGH_00031/2020	3/25/20
MT520187	MA_MGH_00708/2020	4/7/20
MT520188	MA_MGH_00184/2020	3/27/20
MT520189	MA_MGH_00143/2020	3/26/20
MT520190	MA_MGH_00588/2020	3/28/20
MT520191	MA_MGH_00440/2020	3/4/20
MT520192	MA_MGH_00417/2020	3/7/20
MT520193	MA_MGH_00678/2020	3/22/20
MT520194	MA_MGH_00069/2020	3/25/20
MT520195	MA_MGH_00656/2020	4/1/20
MT520197	MA_MGH_00080/2020	3/25/20
MT520198	MA_MGH_00711/2020	4/8/20
MT520199	MA_MGH_00182/2020	3/26/20
MT520200	MA_MGH_00562/2020	3/22/20
MT520201	MA_MGH_00065/2020	3/25/20
MT520202	MA_MGH_00228/2020	4/6/20
MT520203	MA_MGH_00100/2020	3/25/20
MT520205	MA_MGH_00706/2020	4/7/20
MT520207	MA_MGH_00687/2020	4/6/20
MT520208	MA_MGH_00289/2020	4/1/20
MT520209	MA_MGH_00611/2020	3/28/20
MT520211	MA_MGH_00035/2020	3/24/20
MT520212	MA_MGH_00628/2020	3/28/20
MT520213	MA_MGH_00544/2020	3/20/20
MT520214	MA_MGH_00651/2020	4/2/20
MT520215	MA_MGH_00569/2020	3/22/20
MT520217	MA_MGH_00210/2020	3/27/20
MT520220	MA_MGH_00086/2020	3/24/20
MT520221	MA_MGH_00683/2020	3/21/20
MT520223	MA_MGH_00642/2020	4/1/20
MT520224	MA_MGH_00023/2020	3/24/20

MT520225	MA_MGH_00021/2020	3/26/20
MT520226	MA_MGH_00302/2020	4/1/20
MT520227	MA_MGH_00455/2020	4/4/20
MT520228	MA_MGH_00675/2020	4/6/20
MT520229	MA_MGH_00013/2020	3/23/20
MT520231	MA_MGH_00502/2020	3/27/20
MT520233	MA_MGH_00433/2020	3/7/20
MT520237	MA_MGH_00691/2020	4/6/20
MT520240	MA_MGH_00666/2020	4/4/20
MT520241	MA_MGH_00567/2020	3/22/20
MT520242	MA_MGH_00548/2020	3/20/20
MT520249	MA_MGH_00059/2020	3/23/20
MT520253	MA_MGH_00530/2020	3/18/20
MT520254	MA_MGH_00174/2020	3/26/20
MT520255	MA_MGH_00570/2020	3/22/20
MT520257	MA_MGH_00542/2020	3/19/20
MT520258	MA_MGH_00161/2020	3/26/20
MT520259	MA_MGH_00089/2020	3/25/20
MT520261	MA_MGH_00563/2020	3/22/20
MT520263	MA_MGH_00229/2020	4/6/20
MT520265	MA_MGH_00669/2020	4/4/20
MT520266	MA_MGH_00695/2020	4/6/20
MT520267	MA_MGH_00579/2020	3/28/20
MT520268	MA_MGH_00286/2020	4/1/20
MT520269	MA_MGH_00585/2020	3/28/20
MT520271	MA_MGH_00290/2020	4/1/20
MT520272	MA_MGH_00653/2020	4/2/20
MT520273	MA_MGH_00445/2020	4/1/20
MT520274	MA_MGH_00162/2020	3/26/20
MT520275	MA_MGH_00135/2020	3/25/20
MT520279	MA_MGH_00486/2020	3/27/20
MT520280	MA_MGH_00614/2020	3/28/20
MT520281	MA_MGH_00032/2020	3/25/20
MT520282	MA_MGH_00442/2020	3/5/20
MT520283	MA_MGH_00477/2020	4/4/20
MT520284	MA_MGH_00177/2020	3/26/20
MT520286	MA_MGH_00575/2020	3/17/20
MT520290	MA_MGH_00693/2020	4/6/20
MT520291	MA_MGH_00541/2020	3/19/20
MT520293	MA_MGH_00044/2020	3/25/20
MT520294	MA_MGH_00096/2020	3/25/20
MT520295	MA_MGH_00460/2020	4/4/20
MT520296	MA_MGH_00187/2020	3/26/20
MT520297	MA_MGH_00025/2020	3/23/20

MT520299	MA_MGH_00521/2020	3/16/20
MT520301	MA_MGH_00469/2020	4/4/20
MT520303	MA_MGH_00423/2020	3/7/20
MT520305	MA_MGH_00474/2020	4/4/20
MT520306	MA_MGH_00680/2020	3/22/20
MT520307	MA_MGH_00555/2020	3/22/20
MT520311	MA_MGH_00168/2020	3/26/20
MT520313	MA_MGH_00151/2020	3/26/20
MT520314	MA_MGH_00437/2020	3/7/20
MT520317	MA_MGH_00206/2020	3/27/20
MT520321	MA_MGH_00717/2020	4/8/20
MT520322	MA_MGH_00491/2020	3/27/20
MT520326	MA_MGH_00038/2020	3/24/20
MT520329	MA_MGH_00650/2020	4/2/20
MT520330	MA_MGH_00299/2020	4/1/20
MT520331	MA_MGH_00657/2020	4/3/20
MT520334	MA_MGH_00236/2020	4/6/20
MT520335	MA_MGH_00306/2020	4/1/20
MT520338	MA_MGH_00190/2020	3/26/20
MT520339	MA_MGH_00049/2020	3/23/20
MT520340	MA_MGH_00298/2020	4/1/20
MT520342	MA_MGH_00681/2020	3/22/20
MT520343	MA_MGH_00699/2020	4/6/20
MT520344	MA_MGH_00093/2020	3/29/20
MT520345	MA_MGH_00604/2020	3/28/20
MT520346	MA_MGH_00014/2020	3/23/20
MT520347	MA_MGH_00458/2020	4/4/20
MT520348	MA_MGH_00580/2020	3/28/20
MT520351	MA_MGH_00583/2020	3/28/20
MT520352	MA_MGH_00716/2020	4/8/20
MT520353	MA_MGH_00715/2020	4/8/20
MT520354	MA_MGH_00597/2020	3/28/20
MT520355	MA_MGH_00209/2020	3/26/20
MT520360	MA_MGH_00566/2020	3/22/20
MT520362	MA_MGH_00644/2020	4/1/20
MT520363	MA_MGH_00203/2020	3/27/20
MT520364	MA_MGH_00622/2020	3/28/20
MT520365	MA_MGH_00166/2020	3/26/20
MT520366	MA_MGH_00048/2020	3/23/20
MT520368	MA_MGH_00705/2020	4/6/20
MT520369	MA_MGH_00265/2020	4/1/20
MT520372	MA_MGH_00064/2020	3/25/20
MT520376	MA_MGH_00159/2020	3/26/20
MT520378	MA_MGH_00085/2020	3/24/20

MT520379	MA_MGH_00192/2020	3/26/20
MT520380	MA_MGH_00248/2020	4/6/20
MT520381	MA_MGH_00489/2020	3/27/20
MT520384	MA_MGH_00227/2020	4/5/20
MT520386	MA_MGH_00003/2020	3/9/20
MT520387	MA_MGH_00571/2020	3/23/20
MT520389	MA_MGH_00598/2020	3/28/20
MT520390	MA_MGH_00718/2020	4/8/20
MT520391	MA_MGH_00134/2020	3/22/20
MT520392	MA_MGH_00592/2020	3/28/20
MT520393	MA_MGH_00674/2020	4/5/20
MT520395	MA_MGH_00019/2020	3/25/20
MT520396	MA_MGH_00443/2020	3/7/20
MT520398	MA_MGH_00721/2020	4/8/20
MT520399	MA_MGH_00024/2020	3/23/20
MT520402	MA_MGH_00639/2020	4/3/20
MT520404	MA_MGH_00188/2020	3/27/20
MT520405	MA_MGH_00654/2020	4/2/20
MT520406	MA_MGH_00148/2020	3/26/20
MT520407	MA_MGH_00263/2020	4/6/20
MT520410	MA_MGH_00056/2020	3/25/20
MT520411	MA_MGH_00698/2020	4/6/20
MT520412	MA_MGH_00582/2020	3/27/20
MT520413	MA_MGH_00551/2020	3/20/20
MT520414	MA_MGH_00155/2020	3/26/20
MT520415	MA_MGH_00615/2020	3/28/20
MT520418	MA_MGH_00492/2020	3/27/20
MT520419	MA_MGH_00528/2020	3/18/20
MT520423	MA_MGH_00091/2020	3/26/20
MT520424	MA_MGH_00553/2020	3/20/20
MT520425	MA_MGH_00498/2020	3/27/20
MT520428	MA_MGH_00416/2020	3/7/20
MT520429	MA_MGH_00444/2020	3/8/20
MT520431	MA_MGH_00670/2020	4/4/20
MT520437	MA_MGH_00183/2020	3/27/20
MT520438	MA_MGH_00546/2020	3/20/20
MT520439	MA_MGH_00136/2020	3/25/20
MT520440	MA_MGH_00238/2020	4/6/20
MT520442	MA_MGH_00167/2020	3/26/20
MT520443	MA_MGH_00194/2020	3/26/20
MT520444	MA_MGH_00225/2020	3/25/20
MT520445	MA_MGH_00232/2020	4/6/20
MT520449	MA_MGH_00620/2020	3/28/20
MT520450	MA_MGH_00051/2020	3/24/20

MT520451	MA_MGH_00506/2020	3/28/20
MT520455	MA_MGH_00557/2020	3/22/20
MT520456	MA_MGH_00532/2020	3/18/20
MT520457	MA_MGH_00600/2020	3/28/20
MT520458	MA_MGH_00456/2020	4/4/20
MT520461	MA_MGH_00648/2020	4/2/20
MT520462	MA_MGH_00558/2020	3/22/20
MT520463	MA_MGH_00676/2020	3/21/20
MT520466	MA_MGH_00083/2020	3/23/20
MT520468	MA_MGH_00617/2020	3/28/20
MT520470	MA_MGH_00434/2020	3/7/20
MT520471	MA_MGH_00613/2020	3/28/20
MT520472	MA_MGH_00424/2020	3/7/20
MT520473	MA_MGH_00510/2020	3/11/20
MT520474	MA_MGH_00576/2020	3/20/20
MT520476	MA_MGH_00040/2020	3/25/20
MT520477	MA_MGH_00658/2020	4/3/20
MT520480	MA_MGH_00240/2020	4/4/20
MT520484	MA_MGH_00149/2020	3/26/20
MT520486	MA_MGH_00090/2020	3/25/20
MT520487	MA_MGH_00637/2020	4/3/20
MT520489	MA_MGH_00689/2020	4/6/20
MT520490	MA_MGH_00517/2020	3/14/20
MT520491	MA_MGH_00630/2020	4/1/20
MT520492	MA_MGH_00164/2020	3/26/20
MT520493	MA_MGH_00316/2020	4/5/20
MT520496	MA_MGH_00036/2020	3/25/20
MT520497	MA_MGH_00696/2020	4/6/20
MT520498	MA_MGH_00565/2020	3/22/20
MT520499	MA_MGH_00556/2020	3/21/20
MT520500	MA_MGH_00211/2020	3/27/20
MT520502	MA_MGH_00495/2020	3/27/20
MT520503	MA_MGH_00441/2020	3/5/20
MT520505	MA_MGH_00304/2020	4/1/20
MT520511	MA_MGH_00531/2020	3/19/20
MT520512	MA_MGH_00202/2020	3/27/20
MT520513	MA_MGH_00047/2020	3/23/20
MT520514	MA_MGH_00255/2020	4/6/20
MT520519	MA_MGH_00084/2020	3/23/20
MT520520	MA_MGH_00505/2020	3/27/20
MT520522	MA_MGH_00152/2020	3/26/20
MT520523	MA_MGH_00075/2020	3/25/20
MT520524	MA_MGH_00171/2020	3/27/20
MT520526	MA_MGH_00179/2020	3/26/20

MT520527	MA_MGH_00539/2020	3/19/20
MT520528	MA_MGH_00165/2020	3/26/20
MT520529	MA_MGH_00459/2020	4/4/20
MT520531	MA_MGH_00552/2020	3/20/20
MT520532	MA_MGH_00181/2020	3/26/20
MT520533	MA_MGH_00525/2020	3/18/20
MT520534	MA_MGH_00499/2020	3/27/20
MT520535	MA_MGH_00537/2020	3/19/20
MT520537	MA_MGH_00150/2020	3/26/20
MT520540	MA_MGH_00679/2020	3/22/20
MT520541	MA_MGH_00178/2020	3/26/20
MT520542	MA_MGH_00004/2020	3/11/20
MT520543	MA_MGH_00199/2020	3/27/20
MT520544	MA_MGH_00028/2020	3/25/20
MT520545	MA_MGH_00132/2020	3/25/20
MT520546	MA_MGH_00205/2020	3/27/20
MT873050	MA-MGH-01491/2020	5/7/20
MT873051	MA-MGH-01623/2020	5/9/20
MT873052	MA-MGH-00976/2020	5/3/20
MT873053	MA-DPH-00217/2020	4/13/20
MT873054	MA-DPH-00297/2020	4/17/20
MT873055	MA-DPH-00043/2020	4/2/20
MT873056	MA-MGH-00868/2020	4/14/20
MT873057	MA-DPH-00198/2020	4/7/20
MT873058	MA-MGH-01169/2020	4/29/20
MT873059	MA-MGH-01194/2020	5/4/20
MT873060	MA-MGH-00789/2020	4/13/20
MT873062	MA-MGH-00883/2020	4/14/20
MT873063	MA-MGH-01137/2020	5/2/20
MT873064	MA-MGH-01358/2020	5/6/20
MT873066	MA-MGH-00902/2020	4/6/20
MT873069	MA-DPH-00322/2020	4/18/20
MT873070	MA-DPH-00060/2020	4/3/20
MT873072	MA-MGH-01027/2020	4/30/20
MT873073	MA-MGH-01409/2020	5/6/20
MT873074	MA-MGH-01166/2020	4/29/20
MT873075	MA-MGH-00830/2020	4/13/20
MT873076	MA-MGH-01381/2020	5/6/20
MT873077	MA-MGH-01114/2020	5/2/20
MT873078	MA-MGH-01260/2020	5/4/20
MT873079	MA-MGH-01201/2020	5/4/20
MT873080	MA-DPH-00003/2020	3/5/20
MT873081	MA-MGH-01081/2020	5/1/20
MT873083	MA-MGH-01120/2020	5/2/20

MT873085	MA-MGH-00822/2020	4/13/20
MT873087	MA-MGH-01073/2020	4/30/20
MT873089	MA-DPH-00144/2020	4/3/20
MT873090	MA-DPH-00255/2020	4/17/20
MT873091	MA-MGH-01032/2020	5/1/20
MT873092	MA-MGH-01153/2020	4/29/20
MT873094	MA-DPH-00053/2020	4/3/20
MT873095	MA-DPH-00167/2020	4/3/20
MT873096	MA-DPH-00195/2020	4/7/20
MT873098	MA-MGH-01502/2020	5/7/20
MT873099	MA-MGH-00896/2020	5/5/20
MT873101	MA-MGH-01551/2020	4/28/20
MT873106	MA-MGH-00864/2020	4/14/20
MT873107	MA-MGH-00733/2020	4/9/20
MT873108	MA-MGH-01397/2020	5/6/20
MT873109	MA-MGH-00728/2020	4/8/20
MT873111	MA-DPH-00216/2020	4/13/20
MT873112	MA-MGH-01089/2020	5/1/20
MT873113	MA-MGH-00931/2020	5/2/20
MT873114	MA-MGH-00829/2020	4/13/20
MT873115	MA-MGH-01501/2020	5/7/20
MT873116	MA-MGH-00937/2020	5/2/20
MT873118	MA-MGH-00827/2020	4/13/20
MT873121	MA-DPH-00305/2020	4/18/20
MT873122	MA-MGH-01258/2020	5/4/20
MT873125	MA-MGH-01107/2020	5/1/20
MT873127	MA-MGH-01141/2020	5/2/20
MT873129	MA-MGH-01206/2020	5/4/20
MT873131	MA-MGH-01415/2020	5/7/20
MT873132	MA-MGH-00741/2020	4/9/20
MT873133	MA-MGH-01096/2020	5/1/20
MT873134	MA-MGH-01592/2020	5/9/20
MT873136	MA-MGH-00831/2020	4/13/20
MT873137	MA-MGH-00796/2020	4/13/20
MT873138	MA-DPH-00309/2020	4/18/20
MT873140	MA-MGH-01522/2020	5/7/20
MT873142	MA-MGH-01288/2020	5/5/20
MT873143	MA-MGH-01460/2020	4/28/20
MT873144	MA-MGH-01619/2020	5/9/20
MT873146	MA-MGH-00828/2020	4/13/20
MT873147	MA-DPH-00227/2020	4/15/20
MT873148	MA-MGH-00923/2020	5/2/20
MT873149	MA-DPH-00321/2020	4/18/20
MT873150	MA-MGH-00946/2020	5/2/20

MT873152	MA-MGH-01080/2020	5/1/20
MT873154	MA-MGH-00745/2020	4/10/20
MT873155	MA-DPH-00235/2020	4/16/20
MT873156	MA-DPH-00250/2020	4/17/20
MT873159	MA-MGH-01443/2020	4/30/20
MT873160	MA-DPH-00212/2020	4/12/20
MT873161	MA-DPH-00030/2020	4/2/20
MT873162	MA-DPH-00077/2020	4/3/20
MT873163	MA-DPH-00178/2020	4/5/20
MT873164	MA-MGH-01088/2020	5/1/20
MT873166	MA-MGH-00774/2020	4/12/20
MT873167	MA-MGH-01331/2020	5/5/20
MT873170	MA-MGH-01020/2020	4/30/20
MT873171	MA-DPH-00318/2020	4/18/20
MT873173	MA-MGH-00908/2020	4/10/20
MT873174	MA-DPH-00221/2020	4/14/20
MT873175	MA-MGH-01469/2020	5/7/20
MT873178	MA-DPH-00047/2020	4/2/20
MT873180	MA-DPH-00121/2020	4/3/20
MT873182	MA-MGH-01227/2020	5/4/20
MT873184	MA-MGH-00945/2020	5/3/20
MT873185	MA-MGH-00811/2020	4/13/20
MT873186	MA-MGH-00938/2020	5/2/20
MT873187	MA-MGH-01367/2020	5/6/20
MT873189	MA-DPH-00301/2020	4/18/20
MT873191	MA-MGH-01333/2020	5/5/20
MT873192	MA-MGH-01606/2020	5/8/20
MT873193	MA-DPH-00323/2020	4/18/20
MT873194	MA-DPH-00063/2020	4/3/20
MT873196	MA-MGH-00939/2020	5/2/20
MT873197	MA-DPH-00139/2020	4/3/20
MT873201	MA-MGH-01372/2020	5/6/20
MT873202	MA-MGH-00812/2020	4/13/20
MT873203	MA-DPH-00200/2020	4/7/20
MT873205	MA-DPH-00096/2020	4/3/20
MT873206	MA-MGH-00757/2020	4/10/20
MT873208	MA-DPH-00270/2020	4/17/20
MT873209	MA-MGH-01182/2020	4/29/20
MT873210	MA-MGH-00954/2020	5/2/20
MT873211	MA-DPH-00248/2020	4/17/20
MT873214	MA-MGH-01368/2020	5/6/20
MT873215	MA-MGH-01563/2020	5/8/20
MT873216	MA-MGH-01343/2020	5/5/20
MT873219	MA-MGH-00858/2020	4/14/20

MT873223	MA-MGH-01065/2020	5/1/20
MT873225	MA-DPH-00252/2020	4/17/20
MT873227	MA-MGH-01605/2020	5/8/20
MT873229	MA-DPH-00311/2020	4/18/20
MT873232	MA-MGH-00837/2020	4/13/20
MT873234	MA-MGH-00761/2020	4/11/20
MT873235	MA-DPH-00208/2020	4/10/20
MT873237	MA-MGH-01076/2020	5/1/20
MT873238	MA-MGH-00906/2020	4/17/20
MT873239	MA-MGH-01021/2020	4/30/20
MT873241	MA-DPH-00078/2020	4/3/20
MT873242	MA-MGH-01407/2020	5/6/20
MT873243	MA-DPH-00057/2020	4/3/20
MT873244	MA-MGH-00799/2020	4/13/20
MT873245	MA-MGH-01467/2020	5/6/20
MT873246	MA-DPH-00022/2020	4/2/20
MT873248	MA-DPH-00099/2020	4/3/20
MT873250	MA-MGH-01257/2020	5/4/20
MT873251	MA-MGH-00977/2020	5/3/20
MT873252	MA-MGH-00782/2020	4/12/20
MT873253	MA-MGH-01022/2020	4/30/20
MT873255	MA-DPH-00185/2020	4/6/20
MT873256	MA-DPH-00294/2020	4/17/20
MT873257	MA-MGH-01151/2020	4/29/20
MT873259	MA-MGH-01552/2020	4/28/20
MT873260	MA-MGH-00921/2020	5/2/20
MT873262	MA-DPH-00189/2020	4/6/20
MT873264	MA-MGH-01196/2020	5/3/20
MT873265	MA-MGH-01048/2020	5/1/20
MT873267	MA-MGH-00758/2020	4/10/20
MT873268	MA-MGH-00848/2020	4/13/20
MT873270	MA-MGH-01256/2020	5/4/20
MT873271	MA-DPH-00324/2020	4/18/20
MT873272	MA-MGH-00762/2020	4/11/20
MT873273	MA-DPH-00122/2020	4/3/20
MT873275	MA-DPH-00265/2020	4/17/20
MT873276	MA-MGH-01442/2020	4/30/20
MT873278	MA-MGH-01033/2020	4/30/20
MT873280	MA-MGH-00958/2020	5/3/20
MT873281	MA-DPH-00150/2020	4/3/20
MT873285	MA-DPH-00271/2020	4/17/20
MT873288	MA-MGH-00784/2020	4/13/20
MT873289	MA-MGH-00826/2020	4/13/20
MT873290	MA-MGH-01544/2020	4/28/20

MT873291	MA-MGH-01408/2020	5/6/20
MT873293	MA-MGH-00900/2020	5/5/20
MT873295	MA-DPH-00243/2020	4/16/20
MT873297	MA-MGH-00993/2020	4/30/20
MT873298	MA-MGH-00732/2020	4/9/20
MT873299	MA-DPH-00204/2020	4/9/20
MT873300	MA-MGH-01011/2020	4/30/20
MT873301	MA-MGH-01297/2020	5/5/20
MT873302	MA-DPH-00230/2020	4/15/20
MT873305	MA-MGH-00766/2020	4/11/20
MT873306	MA-MGH-00767/2020	4/11/20
MT873310	MA-DPH-00246/2020	4/16/20
MT873312	MA-MGH-01060/2020	5/1/20
MT873313	MA-DPH-00009/2020	3/7/20
MT873315	MA-DPH-00223/2020	4/14/20
MT873316	MA-MGH-01632/2020	4/28/20
MT873317	MA-MGH-01235/2020	5/4/20
MT873321	MA-DPH-00129/2020	4/3/20
MT873322	MA-MGH-00870/2020	4/14/20
MT873324	MA-MGH-01405/2020	5/6/20
MT873325	MA-DPH-00220/2020	4/13/20
MT873328	MA-DPH-00052/2020	4/3/20
MT873330	MA-DPH-00157/2020	4/3/20
MT873332	MA-DPH-00011/2020	3/10/20
MT873334	MA-MGH-01380/2020	5/6/20
MT873335	MA-MGH-01132/2020	5/2/20
MT873337	MA-MGH-00738/2020	4/9/20
MT873338	MA-MGH-01543/2020	4/28/20
MT873339	MA-MGH-00869/2020	4/14/20
MT873340	MA-MGH-00753/2020	4/10/20
MT873341	MA-MGH-01319/2020	5/5/20
MT873343	MA-DPH-00109/2020	4/3/20
MT873344	MA-MGH-00878/2020	4/14/20
MT873346	MA-MGH-01593/2020	5/9/20
MT873348	MA-DPH-00261/2020	4/17/20
MT873350	MA-MGH-01495/2020	5/7/20
MT873351	MA-DPH-00197/2020	4/7/20
MT873352	MA-MGH-00871/2020	4/14/20
MT873353	MA-MGH-00764/2020	4/11/20
MT873354	MA-MGH-01350/2020	5/6/20
MT873355	MA-DPH-00256/2020	4/17/20
MT873356	MA-DPH-00090/2020	4/3/20
MT873357	MA-MGH-00873/2020	4/14/20
MT873358	MA-DPH-00257/2020	4/17/20

MT873360	MA-MGH-00760/2020	4/10/20
MT873361	MA-MGH-01338/2020	5/5/20
MT873363	MA-MGH-00740/2020	4/9/20
MT873365	MA-MGH-00817/2020	4/13/20
MT873367	MA-MGH-01045/2020	5/1/20
MT873368	MA-MGH-00916/2020	5/2/20
MT873369	MA-DPH-00209/2020	4/10/20
MT873370	MA-MGH-01304/2020	5/5/20
MT873371	MA-MGH-01145/2020	5/2/20
MT873372	MA-MGH-00947/2020	5/2/20
MT873375	MA-MGH-00926/2020	5/2/20
MT873376	MA-MGH-01108/2020	5/2/20
MT873378	MA-MGH-00734/2020	4/9/20
MT873380	MA-MGH-00816/2020	4/13/20
MT873381	MA-MGH-00959/2020	5/3/20
MT873384	MA-MGH-01057/2020	5/1/20
MT873386	MA-DPH-00037/2020	4/2/20
MT873388	MA-DPH-00066/2020	4/3/20
MT873389	MA-MGH-00992/2020	5/1/20
MT873390	MA-DPH-00124/2020	4/3/20
MT873391	MA-MGH-01504/2020	5/7/20
MT873394	MA-DPH-00010/2020	3/7/20
MT873395	MA-DPH-00306/2020	4/18/20
MT873396	MA-MGH-01121/2020	5/2/20
MT873397	MA-MGH-01382/2020	5/6/20
MT873398	MA-DPH-00028/2020	4/2/20
MT873399	MA-DPH-00238/2020	4/16/20
MT873400	MA-MGH-01387/2020	5/6/20
MT873402	MA-DPH-00158/2020	4/3/20
MT873406	MA-MGH-01586/2020	5/9/20
MT873407	MA-MGH-01344/2020	5/5/20
MT873408	MA-MGH-01207/2020	5/4/20
MT873410	MA-MGH-01452/2020	4/30/20
MT873412	MA-MGH-01017/2020	4/30/20
MT873415	MA-DPH-00313/2020	4/18/20
MT873416	MA-DPH-00202/2020	4/8/20
MT873420	MA-MGH-01071/2020	4/30/20
MT873423	MA-MGH-01070/2020	5/1/20
MT873425	MA-DPH-00186/2020	4/6/20
MT873427	MA-DPH-00086/2020	4/3/20
MT873430	MA-MGH-01157/2020	4/29/20
MT873431	MA-DPH-00051/2020	4/2/20
MT873432	MA-MGH-00788/2020	4/13/20
MT873433	MA-MGH-01365/2020	5/6/20

MT873434	MA-DPH-00268/2020	4/17/20
MT873435	MA-DPH-00044/2020	4/2/20
MT873436	MA-DPH-00163/2020	4/3/20
MT873439	MA-DPH-00089/2020	4/3/20
MT873441	MA-DPH-00031/2020	4/2/20
MT873443	MA-DPH-00283/2020	4/17/20
MT873444	MA-DPH-00083/2020	4/3/20
MT873446	MA-DPH-00229/2020	4/15/20
MT873447	MA-MGH-01448/2020	4/30/20
MT873449	MA-MGH-01119/2020	5/2/20
MT873454	MA-DPH-00095/2020	4/3/20
MT873455	MA-DPH-00134/2020	4/3/20
MT873456	MA-MGH-00887/2020	4/14/20
MT873457	MA-DPH-00236/2020	4/16/20
MT873459	MA-MGH-00903/2020	4/8/20
MT873460	MA-DPH-00035/2020	4/2/20
MT873461	MA-MGH-01161/2020	4/29/20
MT873462	MA-DPH-00062/2020	4/3/20
MT873471	MA-MGH-00775/2020	4/12/20
MT873472	MA-MGH-01110/2020	5/1/20
MT873474	MA-DPH-00120/2020	4/3/20
MT873475	MA-MGH-01271/2020	4/29/20
MT873478	MA-DPH-00155/2020	4/3/20
MT873480	MA-DPH-00048/2020	4/2/20
MT873481	MA-MGH-01471/2020	5/6/20
MT873482	MA-MGH-00855/2020	4/13/20
MT873483	MA-MGH-01580/2020	5/8/20
MT873485	MA-MGH-00814/2020	4/13/20
MT873486	MA-MGH-00840/2020	4/13/20
MT873488	MA-MGH-00866/2020	4/14/20
MT873490	MA-MGH-01248/2020	5/4/20
MT873492	MA-MGH-00768/2020	4/11/20
MT873494	MA-MGH-01329/2020	5/5/20
MT873495	MA-DPH-00263/2020	4/17/20
MT873497	MA-DPH-00002/2020	3/3/20
MT873500	MA-MGH-00773/2020	4/12/20
MT873502	MA-DPH-00171/2020	4/3/20
MT873503	MA-MGH-00886/2020	4/14/20
MT873506	MA-DPH-00192/2020	4/6/20
MT873508	MA-DPH-00055/2020	4/3/20
MT873509	MA-MGH-00853/2020	4/13/20
MT873510	MA-MGH-00730/2020	4/9/20
EPI_ISL_456115	NY-NYUMC843/2020	5/3/20
EPI_ISL_467377	NY-NYUMC884/2020	5/3/20

EPI_ISL_467379	NY-NYUMC886/2020	5/8/20
EPI_ISL_467384	NY-NYUMC891/2020	5/10/20
EPI_ISL_467386	NY-NYUMC893/2020	5/8/20
EPI_ISL_467390	NY-NYUMC897/2020	5/9/20
EPI_ISL_467400	NY-NYUMC907/2020	5/7/20
EPI_ISL_467403	NY-NYUMC910/2020	5/7/20
EPI_ISL_467404	NY-NYUMC911/2020	5/7/20
EPI_ISL_467405	NY-NYUMC912/2020	5/8/20
EPI_ISL_467406	NY-NYUMC913/2020	5/7/20
EPI_ISL_467407	NY-NYUMC914/2020	5/8/20
EPI_ISL_467408	NY-NYUMC915/2020	5/8/20
EPI_ISL_495497	WI-UW-793/2020	7/5/20
EPI_ISL_526686	NY-MH001867/2020	5/10/20
EPI_ISL_526688	NY-MH001832/2020	5/6/20
EPI_ISL_452145	CT-Yale-333/2020	5/12/20
EPI_ISL_484972	NY-UW-597/2020	6/27/20
EPI_ISL_491316	MA-UW-633/2020	6/27/20
EPI_ISL_421584	NJ-NYUMC83/2020	3/18/20
EPI_ISL_421389	NY-PV08434/2020	3/18/20
EPI_ISL_418973	NY-NYUMC27/2020	3/17/20
EPI_ISL_414476	NY1-PV08001/2020	2/29/20
EPI_ISL_415151	NY2-PV08100/2020	3/4/20
EPI_ISL_418977	NY-NYUMC31/2020	3/17/20
EPI_ISL_409067	MA1/2020	1/29/20
EPI_ISL_427161	CT-UW-3845/2020	3/25/20
EPI_ISL_424174	CT-UW-1365/2020	3/13/20

ACKNOWLEDGEMENTS

First and foremost, we are profoundly grateful to this patient and his family for their kindness, generosity, and the innumerable lessons that he taught us throughout his life. We thank Rebecca Zaffini, Mischa Covington, and other members of the Clinical Microbiology Laboratory at Brigham and Women's Hospital (BWH) and Drs. Daimon Simmons and Nicole Tolan of the Department of Pathology at BWH for their assistance and expertise. We acknowledge Jacob Plaisted of the Autopsy Division of the BWH Department of Pathology for his dedication and expertise in safely performing the technical aspects of the autopsy. We appreciate the assistance of the BWH Center for Clinical Investigation and the Mass General Brigham Biobank. Lastly, we thank the physicians, physician assistants, nurses, respiratory therapists, custodial staff, and other team members that participated in the care of this patient.

SUPPLEMENTAL REFERENCES

1. Martinot M, Jary A, Fafi-Kremer S, et al. Remdesivir failure with SARS-CoV-2 RNA-dependent RNA-polymerase mutation in a B-cell immunodeficient patient with protracted Covid-19. Clin Infect Dis 2020 Sep 28 (Epub ahead of print).
2. Baang JH SC, Mirabelli C, Valesano AL, et al. Prolonged SARS-CoV-2 replication in an immunocompromised patient. 2020 Sep 22 (https://www.medrxiv.org/content/10.1101/2020.09.20.20196899v1) Preprint.
3. Tillett RL SJ, Hartley PD, Kerwin H, et al. Genomic evidence for reinfection with SARS-CoV-2: a case study. Lancet 2020 Oct 12 (Epub ahead of print).
4. Mulder M, Van Der Vegt DSJM, Oude Munnink BB, et al. Reinfection of SARS-CoV-2 in an immunocompromised patient: a case report. Clinical Infectious Diseases 2020 Oct 9 (Epub ahead of print).
5. Fact sheet for health care providers: Emergency use authorization (EUA) of Veklury® (remdesivir). Silver Spring, MD: The U.S. Food and Drug Administration (FDA), August 2020. (https://www.fda.gov/media/137566/download).
6. Baum A, Fulton BO, Wloga E, et al. Antibody cocktail to SARS-CoV-2 spike protein prevents rapid mutational escape seen with individual antibodies. Science 2020;369:1014-8.
7. Deane KD, West SG. Antiphospholipid Antibodies as a Cause of Pulmonary Capillaritis and Diffuse Alveolar Hemorrhage: A Case Series and Literature Review. Seminars in Arthritis and Rheumatism 2005;35:154-65.
8. Cervera R, Piette J-C, Font J, et al. Antiphospholipid syndrome: Clinical and immunologic manifestations and patterns of disease expression in a cohort of 1,000 patients. Arthritis & Rheumatism 2002;46:1019-27.
9. Wölfel R, Corman VM, Guggemos W, et al. Virological assessment of hospitalized patients with COVID-2019. Nature 2020;581:465-9.
10. He X, Lau EHY, Wu P, et al. Temporal dynamics in viral shedding and transmissibility of COVID-19. Nat Med 2020;26:672-5.
11. Yonker LM, Neilan AM, Bartsch Y, et al. Pediatric SARS-CoV-2: Clinical Presentation, Infectivity, and Immune Responses. The Journal of Pediatrics 2020:S0022347620310234.
12. Elbe S, Buckland-Merrett G. Data, disease and diplomacy: GISAID's innovative contribution to global health. Glob Chall 2017;1:33-46.
13. Research Use Only 2019-Novel Coronavirus (2019-nCoV) Real-time RT-PCR Primers and Probes. Atlanta, GA: Centers for Disease Control and Prevention, April 2020. (https://www.cdc.gov/coronavirus/2019-ncov/downloads/rt-pcr-panel-primer-probes.pdf).
14. Fajnzylber JM, Regan J, Coxen K, et al. SARS-CoV-2 Viral Load is Associated with Increased Disease Severity and Mortality. 2020 Jul 17 (https://www.medrxiv.org/content/10.1101/2020.07.15.20131789v1) Preprint.
15. Yonker LM, Neilan AM, Bartsch Y, et al. Pediatric SARS-CoV-2: Clinical Presentation, Infectivity, and Immune Responses. J Pediatr 2020 Aug 20 (Epub ahead of print).
16. Palmer S, Wiegand AP, Maldarelli F, et al. New real-time reverse transcriptase-initiated PCR assay with single-copy sensitivity for human immunodeficiency virus type 1 RNA in plasma. J Clin Microbiol 2003;41:4531-6.
17. Gonzalez-Reiche AS, Hernandez MM, Sullivan MJ, et al. Introductions and early spread of SARS-CoV-2 in the New York City area. Science 2020;369:297-301.
18. nCoV-2019 sequencing protocol v1. 2020. at https://www.protocols.io/view/ncov-2019-sequencing-protocol-bbmuik6w.
19. Shepard SS, Meno S, Bahl J, Wilson MM, Barnes J, Neuhaus E. Viral deep sequencing needs an adaptive approach: IRMA, the iterative refinement meta-assembler. BMC Genomics 2016;17:708.
20. Katoh K, Rozewicki J, Yamada KD. MAFFT online service: multiple sequence alignment, interactive sequence choice and visualization. Brief Bioinform 2019;20:1160-6.
21. Trifinopoulos J, Nguyen LT, von Haeseler A, Minh BQ. W-IQ-TREE: a fast online phylogenetic tool for maximum likelihood analysis. Nucleic Acids Res 2016;44:W232-5.
22. Harcourt J, Tamin A, Lu X, et al. Severe Acute Respiratory Syndrome Coronavirus 2 from Patient with Coronavirus Disease, United States. Emerg Infect Dis 2020;26:1266-73.
23. Brown EP, Licht AF, Dugast AS, et al. High-throughput, multiplexed IgG subclassing of antigen-specific antibodies from clinical samples. J Immunol Methods 2012;386:117-23.